Doctoral Dissertation

Kinetics in Solid State Bonding of Superplastic Steel and Bonding Mechanism Analysis

Zhonghao Heng

December 2015

Graduate School of Engineering

Osaka University

Kinetics in Solid State Bonding of Superplastic Steel and the Bonding Mechanism Analysis

Chapter 1: Introduction

1.1 Superplasticity Behaviors

1.1.1 Definition of Superplasticity and Superplastic Materials

Superplasticity, the ability of certain materials to undergo very large tensile strains, was first described by Bengough in 1912 [1]. It became a popular research topic in the early 1960s following a review article by Underwood [2] and development of the potential commercial application of superplasticity.

However, there has been no generally accepted definition of all time for superplasticity. The following version was proposed and accepted after deliberation at the 1991 International Conference on Superplasticity in Advanced Materials (ICSAM-91) held in Osaka, Japan [3,4]:

"Superplasticity is the ability of polycrystalline material to exhibit, in a generally isotropic manner, very high tensile elongations prior to failure."

In general, it can be called superplasticity when the tensile elongation δ is over 100 percent. For some superplastic materials, the tensile elongation can actually reach to several hundred percent. An elongation to failure of 8000% in commercial bronze was reported in 1992 by K. Higashi [5].

With a further research on superplasticity behavior, materials shown to exhibit superplasticity are extended to ceramics and intermetallic since 1985 and 1987 respectively [6]. These superplastic materials can just show superplasticity behaviors under appropriate conditions, especially the deformation conditions.

1.1.2 Evaluation Indexes

Phenomenologically, the tensile deformation characteristic prior to fracture of certain alloys in the state of superplasticity can be described by large deformation, low flow stress, and neck-free [4, 7]. Furthermore, superplastic materials generally exhibit high value of the strain rate sensitivity exponent *m* during superplastic deformation, which is characterized by the constitutive equation proposed by Backofen [8]:

$$\sigma = k\dot{\varepsilon}^m \tag{1-1}$$

where σ is the flow stress, k is a constant, and $\dot{\varepsilon}$ is the strain rate. Newtonian viscous behavior occurs in materials, such as molasses and glass, when $m = 1$. In general, most metals and alloys normally have values of $m < 0.2$ whereas superplastic materials can typically exhibit $m > 0.3$. In other hand, superplasticity behavior is found when $m > 0.3$, and the higher value of *m*, the lower rate of reducing of cross-section, the more stable uniform tensile deformation, the larger elongation. The major evaluation indexes on superplasticity behavior are elongation δ, strain rate sensitivity exponent *m*, and also the deformation activation energy *Q* [4, 9-10].

The equation for superplastic deformation under constant stress proposed by Mukherjee [11] is expressed by

$$\dot{\varepsilon} = \left[\frac{AD_0Gb}{kT}\left(\frac{b}{d}\right)^p\left(\frac{\sigma}{G}\right)^n\right]\exp\left(-\frac{Q}{RT}\right), \tag{1-2}$$

and the diffusion coefficient *D* is expressed by

$$D = D_0 \exp\left(-\frac{Q}{RT}\right), \tag{1-3}$$

where A is a constant; G is the shear modulus; b is Burgers vector; k is Boltzmann's constant; d is the average grain size; p is the index of grain size; n is the stress exponent; D_0 is the frequency factor, the value of D when $T = \infty$; R is the gas constant; and T is the thermodynamic temperature. When the value in the square brackets is supposed as a constant, the value of Q can be obtained by

$$Q = -R\left[\frac{\partial \ln \dot{\varepsilon}}{\partial (1/T)}\right]. \tag{1-4}$$

Because the superplastic flow is essentially a grain boundary phenomenon, the Q value for superplastic deformation should be close to that of interfacial (or grain boundary) self-diffusion, Q_b, as described in the following chapter [4, 12-15].

1.1.3 Fine-structure Superplasticity

There are two well-established types of superplasticity behavior in polycrystalline solids: fine-structure superplasticity (FSS) and internal-stress superplasticity (ISS) [4]. The first type of superplasticity, also known as isothermal superplasticity, is the best known and the most studied. The second type of superplasticity behavior is known as ISS or phase-transformation superplasticity. In this case, polymorphic materials should present the phase change through thermal cycling or pressure cycling, and the fine

structure is not a necessary condition [16-20]. However, the application of ISS is greatly limited due to the complicated prerequisite of temperature and pressure.

The present research focuses exclusively on the first type of superplasticity, which is FSS. Some necessary prerequisites are given for FSS materials. Firstly, the grain size should be small for a grain boundary sliding mechanism to dominate superplastic deformation. Typically, the grain size for metal-based materials should be less than 10μm. A finer grain size increases the strain rate for superplasticity flow in general [9]. Secondly, the shape of grains should be equiaxed to enable the occurrence of grain boundary sliding which provide by a shear stress along grain boundaries. Furthermore, the presence of a second phase is also required to restrict grain growth at superplastic temperatures at which grain-boundary sliding occurs [4, 21-22]. Superplasticity is usually improved if the grain size is steady due to the fine second phase and its uniform distribution. Therefore, as an evaluation indexes, the activation energy of FFS controlled by grain-boundary sliding must be equal to Q_b or less than Q_b [9, 12-15, 23]. In conclusion, materials with a fine, equiaxed, two-phase structure can show superplasticity (FSS) under appropriate deformation conditions.

1.2 Solid State Bonding

Welding processes can be classified into two main categories: liquid phase welding and solid state welding [24]. In the former case, bonds are established by the formation and solidification of a liquid phase at the interface while, in the latter case, the coalescence is produced at temperatures essentially below the melting point of the base materials

being joined and the applied pressure has a key role in bringing together the surfaces to be joined within interatomic distance [25].

1.2.1 Solid State Diffusion Bonding

Solid state bonding is often used as a synonym for solid state diffusion bonding [26]. Indeed, it is merely a type of solid-state welding, along with forge welding, friction welding, and explosive welding. A modified definition of solid state diffusion bonding, proposed by Kazakov [24], is described as following: solid state diffusion bonding of materials is a process for making a monolithic joint through the formation of bonds at atomic level, as a result of closure of the mating surfaces due to the local plastic deformation at elevated temperature which aids inter-diffusion (an accompanying phenomena during bonding, but not necessary for the bonding process [25]) at the surface layers of the materials being joined. In the present study, the expression of solid state bonding is adopted.

Solid state bonding process, as an important mean of achieving high quality and precision joining of dissimilar materials, needs at least two main stages: interfacial contact (or void shrinkage at the bond interface) and chemical binding at the contact area [24, 25, 27]. Thermally activated mechanisms such as dislocation creep deformation and vacancy diffusion (an atom flux along the bonding interface and void surface) lead to interfacial contact process and this controls the bonding process as a determining step [25, 28-30].

1.2.2 Modeling of Solid State Bonding

Table 1.1 Models of solid state bonding.

Timeline	Models	Ref.	Characteristics
1966	Cline	[32]	A two-stage model assuming localized plastic deformation followed by the diffusion-controlled process, using the recrystallization model of Parks (1953) [33].
1967	King and Owezarski	[34]	A three-stage model similar to Cline's model, the migration of interface away from the voids was assumed to occur during the second stage and the remaining isolated voids are removed by volume diffusion in the third stage.
1975	Garmong et al.	[35]	Similar to the Hamilton's model but including diffusion mechanisms. Removal of the voids was modelled by using the sintering equations derived by Coble (1970).
1982	Derby and Wallach	[36]	Based on an intensive use of the sintering equations assuming six different diffusion mechanisms.
1984	Derby and Wallach	[37]	Modification of the previous model (1982) in order to reduce the existing discontinuity in bonding rate between the second and final stage.
1984	Pilling et al.	[38]	A diffusion creep cavitation model adopted for fine grain superplastic alloys based on creep model of Chen and Argon (1981) [39].
1984	Nishigushi and Takahashi	[40]	A two dimensional model for solid state bonding process and the bonding process is assumed to be achieved by four distinguishable mechanisms.
1987	Guo and Ridley	[41]	Using the same mechanisms as the Derby and Wallach model but assuming two mechanisms act in parallel.
1989	Hill and Wallach	[42]	Assuming elliptic voids with successive incremental changes in shape to circular and two concomitant modes.
1992	Takahashi and Inoue	[43]	An overview of the void shrinkage models including the model proposed by Takahashi (1988&1991) based on diffusion flow of atoms and successive mechanisms for $D_s >> D_b$.
1995	Takahashi and Tanimoto	[44]	Finite elements analysis of interfacial contact process due to power law creep and no diffusion mechanisms are taken into account.

In physical terms, the bonding process can be best portrayed as the sintering of a planar array of voids at high temperature. Derby and Wallach [31] predicted that the principal mechanism by which the voids close is that of power law creep, i.e. plastic flow rather than diffusion. That is also why the bonding process is more accurately described as solid state bonding rather than diffusion bonding [38]. To optimize the process variables such as surface asperity, bonding temperature, pressure, and time, modeling solid state bonding is attempted, and thus to obtain a reasonable and profound understanding of the bonding mechanisms and their relative contribution not only for different bonding conditions but also for different materials being joined. A chronological summary of the proposed models is shown in Table 1.1. Derby and Wallach were the first to combine multiple mechanisms during the bonding process. Since then, all existing models of solid state bonding, for a metal-metal bond in general, take into account both creep mechanism and diffusional mechanism [36, 43]. In the present study, the solid state bonding of superplastic materials is further investigated based on the existing models.

1.2.3 Solid State Bonding of Superplastic Materials

Superplastic materials often show extremely large deformability and strong diffusion when deformed in superplastic mode. Therefore, the intimate contact can be achieved more efficiently than conventional creep deformation. In other words, fine grained materials can be readily bonded in the solid state due to the enhancement on interfacial contact process by superplastic flow [4, 13-15, 45].

This type of bonding, which is based on the superplasticity of bonding materials, has

attracted increasing concern. For instance, concurrent superplastic forming and diffusion bonding (SPF/DB) developed by Rockwell since 1970s has been recognized as a viable manufacturing technology that can result in both cost and weight savings compared with conventional bonding methods [4, 46-49]. Up to the present, SPF/DB of superplastic titanium alloy is successfully applied in the fabrication of aerospace structures and it is of great value in technical and economic benefits. In addition, superplastic materials such as aluminum alloys (Supral100 and Supral220) and ultrahigh carbon (UHC) steel can be used to produce laminated composites by solid state bonding [50, 51]. This type of laminated composites with sharp interfaces between layers have been shown to exhibit unusual impact, toughness, and combination properties. Furthermore, the friction stir welding (FSW) of superplastic aluminum alloys such as AA2095 has also be researched by H.G. Salem [52]. It can be confirmed that joint after bonding can still maintain high strength and superplastic characteristics. FSW based on superplastic flow is also expected to be applied to the poor weldability materials such as steel and iron materials.

Table 1.2 Chemical components of superplastic steels.

Steel	Chemical components					
	C	Cr	Mn	Si	V	Ni
40Cr	0.37~0.45	0.8~1.1	0.5~0.8	0.17~0.37	-	-
T10	0.95~1.04	-	≤ 0.40	≤ 0.35	-	-
Cr12MoV	1.45~1.70	11.0~12.5	≤ 0.40	≤ 0.40	0.15~0.30	≤ 0.25
SUS329J1	≤0.15	17.0~19.0	≤ 2.00	≤ 1.00	-	8.0~10.0
UHC steel	1.60	1.54	0.44	0.49	-	-

Notes: All the superplastic steels shown in this table are in Chinese standard. 40Cr is the carbon steel (SCr40 in JIS). T10 is the tool steel (Sk105 in JIS). SUS329J1 is the ferritic stainless steel.

Solid state bonding of superplastic materials has been experimentally demonstrated to be more efficient than conventional DB without superplasticity, especially for the structural steels and ferrous alloys [4, 45]. A summary of the previous study on solid state bonding of fine grain superplastic steels (shown in Table 1.2) is given in Table 1.3.

Table 1.3 Solid state bonding of superplastic steels.

Material	Bonding parameters					Joint strength	Ref.
	atmosphere	Pre-stress MPa	Bonding temperature T/℃	Initial strain rate $\dot{\varepsilon}$ / $\times 10^{-4}$/s	Bonding time t/s		
40Cr	-	35	730~780	1.7~4.2	180~300	same with parent metal	[53]
T10	-	40	750~780	1.7~2.5	180~300	same with parent metal	[53]
40Cr / T10	-	40~90	760~780	1.7~2.5	180~300	same with 40Cr	[53-56]
40Cr / Cr12MoV	-	50~100	750~800	2.5	180~480	close to 40Cr	[57]
QCr0.5 / 40Cr	-	40~70	750~800	2.5~7.5	120~180	close to QCr0.5	[58]
SUS329J1 stainless steel	vacuum	9.5	900~1100		120	same with parent metal	[59]
UHC steel / 40Cr	-	50	750~820	1.5~3	300~600	540 MPa	[60-61]

Bonding parameters, particularly temperatures and pressures, adopted during bonding, are within the range for superplasticity in materials. Zhang and coworkers [53-58, 60-61] reported significant results on DB using the superplasticity of high carbon steels at temperatures around the A_1 point (eutectoid temperature) and high quality bonding was performed in several minutes without protective atmosphere or vacuum. Heng [62-64] found that the weldability of superplastic UHC steel can be improved further by improving the microstructure via an appropriate interlayer.

Although typical and uniform superplastic flow has been observed in parent metal, the plastic flow contributed to the interfacial contact has not been distinguished clearly yet. The solid state bonding of superplastic materials is not conceptually be the same as superplastic bonding. In other words, superplastic bonding can be established only when the superplastic flow mainly leads to the interfacial contact. There is no doubt that superplastic flow can facilitate the interfacial contact at the beginning of bonding process [4, 13-15, 45]. In addition, the grain size of superplastic material being bonded is substantially less than the void size/surface roughness and hence more grain boundaries would be involved in mass transfer to close the void [4]. The void shrinkage rate can be correspondingly increased even in the late stage of bonding. However, the predominant bonding mechanisms, including the effect of superplastic flow, are not fully understood yet. Further investigation of interfacial contact is needed to demonstrate the facilitation of superplastic flow and quantify its effect on the bonding process.

1.3 Objective and Flow of the Present Study

Up to the present, many studies have been devoted to the mechanistic description of solid state bonding, especially to the kinetics of void shrinkage at the bonding interface. It is generally known that various high-temperature deformation, such as power law creep, and diffusional creep, predominantly contribute to the interfacial contact process during different bonding stages under the influence of bonding parameters and surface conditions, especially surface roughness. Furthermore, the identification model established by Takahashi [25, 30] can well distinguish the predominant bonding mechanisms at different bonding stage, thus optimizing the bonding process.

For superplastic materials, it is expected that superplastic flow can play a major role during the bonding process. Because of superplastic flow, the requirements of surface finish and atmosphere decrease and more efficient bonding can be obtained under relatively low stress in a short time. Current researches [50-64] on solid state bonding with superplasticity primarily focus on the attempt to optimize the bonding parameters and then the proper bonding conditions can be determined. However, the basic understanding of superplastic effect on the bonding process and predominant bonding mechanisms are still limited. A more complete description of solid state bonding should be established on the base of kinetics of interfacial contact process and superplasticity behavior.

In the present study, the solid state bonding of fine grained high carbon steel SK105 with different surface roughness is investigated using the existing identification model proposed by Takahashi [30]. There are three main research objectives as following: (1) to enrich the description of existing model of solid state bonding, (2) to qualitatively

evaluate the effect of superplastic deformation on the bonding process, and (3) to develop a novel efficient solid state bonding technique based on the maximum use of superplasticity behavior.

More specifically, it is rarely reported that superplastic flow can be predominant at a certain stage, so the first purpose is to get a better understanding of solid state bonding of superplastic materials by identifying the predominant bonding mechanisms during different bonding stage. Secondly, superplastic solid state bonding can be confirmed by the interfacial deformation behavior and the microstructure characteristics. The effect of superplasticity can also be qualitatively described. Based on the understanding above, the prerequisite bonding conditions, which is essential for superplastic solid state bonding can be identified. Further, to realize the application, the bonding process in which superplastic flow is predominant can be extended by optimizing the bonding parameters and hence more efficient solid state bonding with superplasticity can be developed.

This thesis consists of six chapters. Fig. 1.1 shows the flow of the present study. In Chapter 1, a brief introduction to the superplasticity, solid state bonding of superplastic materials, and the purpose of the present study is given. In Chapter 2, the theories of creep deformation and identification of predominant bonding mechanisms are described to provide a theoretical model. In Chapter 3, the preparation of superplastic steel and the experimental conditions are described. In Chapter 4, and 5, the bonding process controlled by creep deformation, including power law creep, superplastic flow, and diffusional creep, are described in detail. The value of stress exponent n and activation energy Q are adopted to identify the predominant bonding mechanisms respectively. The influence of surface roughness is also discussed. In Chapter 6, the

conclusion of the present study and the further research plans are described in detail.

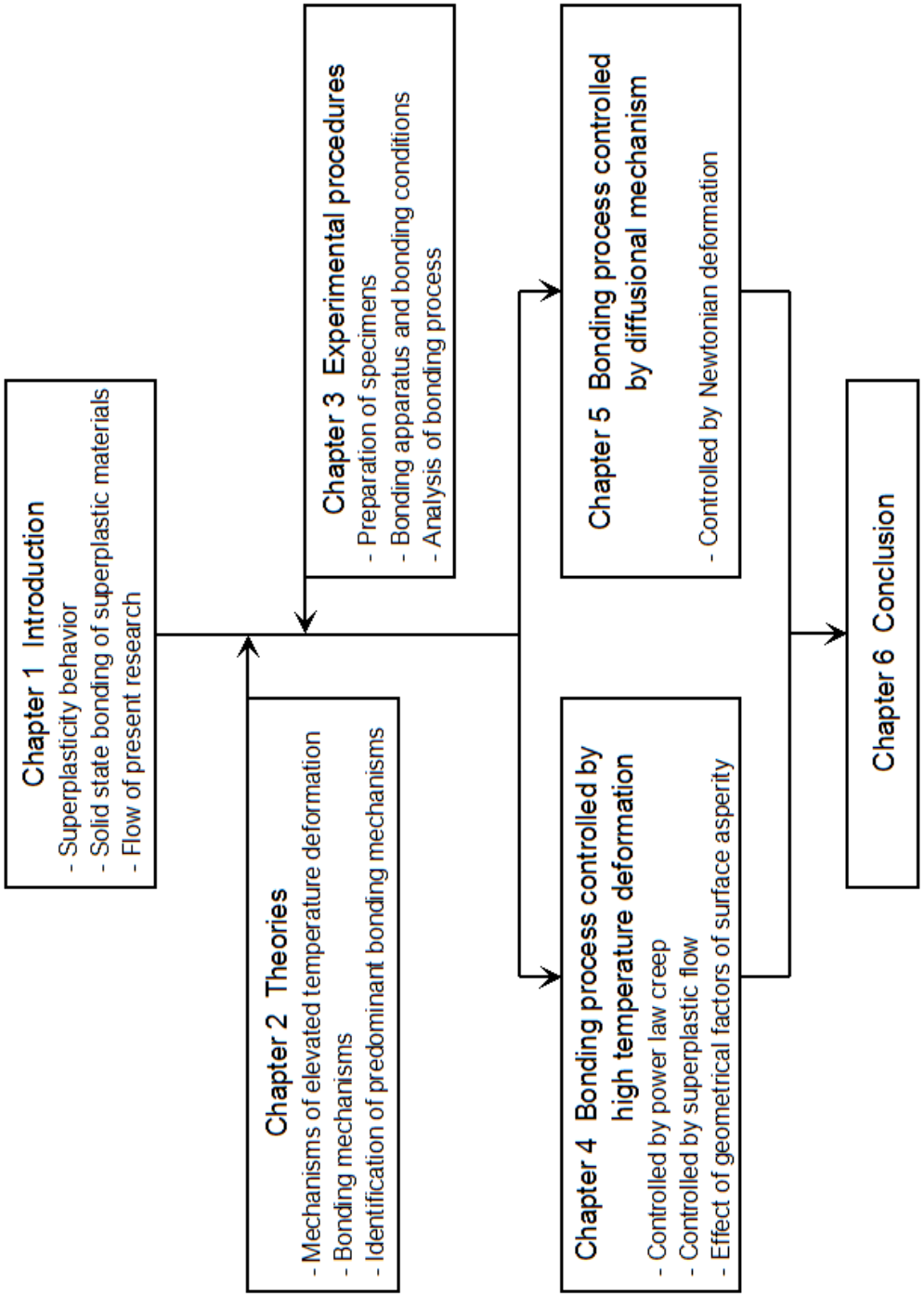

Fig. 1.1 Flow of the present study.

References

[1] G. D. Bengough: J. Inst. Metals., 1912, Vol. 8, pp. 123-174.

[2] E. E. Underwood: J. Metals., 1962, Vol. 14, pp. 914-919.

[3] S. Hori, M. Tokizane and N. Furushiro: Superplasticity in Advanced Materials., 1991, Osaka, Japan.

[4] T. G. Nieh: Superplasticity in Metals and Ceramics., 1997, Cambridge University Press, New York.

[5] K. Higashi, Unpublished Research, University of Osaka prefecture. 1992, Osaka, Japan.

[6] C. Carry and A. mocellin: High Ductilities in Fine Grained Ceramics, 1985, Centre National de la Recherché Scientifique, Paris, France, pp. 16.1-16.19.

[7] T. G. Langdon: Metall. Trans., 1982, Vol. 13, pp. 689-701.

[8] W. A. Backofen: ASM. Trans. Quart., 1964, Vol. 57, pp. 980-990.

[9] O. D. Sherby and J. Wadsworth: ASM, Metal Park., 1984, ASM, Metal Park, Ohio, pp. 355-389.

[10] W. B. Morrison: ASM Trans. Quart., 1968, Vol. 61, pp. 423.

[11] A. K. Mukherjee: High Temperature Creep., 1975, Academic Press, New York, pp. 163-170.

[12] RC. Gifkins: Metall Trans., 1976, Vol. 7, pp. 1225.

[13] Z.H. Heng, M. Maeda and Y. Takahashi: IOP Conf. Series: Mater. Sci. Eng., Doc.No. 61(2014)012003.

[14] Z.H. Heng, T. Matsushima, Y. Nashiki, M. Maeda, K.K. Zhang and Y. Takahashi:

Quarterly Journal of the Japan Welding Society., 2015, Vol. 33(2), pp. 67-70.

[15] Z.H. Heng, T. Matsushima, Y. Nashiki, M. Maeda and Y. Takahashi: Journal of Smart Processing., 2015, Vol. 4, pp. 102-108.

[16] M. Jong and G. W. Rathenau: Acta Metall., 1961, Vol. 9, pp. 714-720.

[17] O. A. Ruano, J. Wadsworth and O. D. Sherby: Metall. Trans., 1982, Vol. 13, pp. 355-361.

[18] L. A. Xue and R. Raj: J. Am. Ceram. Soc., 1989, Vol. 72, pp. 1792-1796.

[19] Y. Maehara and T. G. Langdon: J. Mater. Rev., 1990, Vol. 25, pp. 2275-2286.

[20] T. G. Nieh, J. Wadsworth and F. Wakai: Inter. Mater. Rev., 1991, Vol. 36(4), pp. 146-161.

[21] J. W. Chuang and J. R. Cahoon: Metal. Sci., 1979, Vol. 13, pp. 635-640.

[22] Y. Maehara: Trans. ISIJ., 1987, Vol. 27, pp. 705-712.

[23] H. Fukuyo, H. C. Tsai, T. Oyama and O. D. Sherby: ISIJ International., 1991, Vol. 31(1), pp. 76-85.

[24] N. F. Kazakov: Diffusion Bonding of Materials., 1985, Pergamon Press, Oxford.

[25] Y. Takahashi: Ceramic Trans., 2003, Vol. 138, pp. 29-47.

[26] H. Y. Wu, S. Lee and J. Y. Wang: J. Mater. Process. Technol., 1998, Vol. 75, pp. 173-179.

[27] K.Saida: Journal of the Japan Society for Precision Engineering., 2011, Vol. 77(3), pp. 273-277. (in Japanese)

[28] Y. Takahashi and M.Tanimoto: Trans. ASME J. Eng. Mater. Technol., 1995, Vol. 117, pp. 336-340.

[29] Y. Takahashi and M.Tanimoto: Trans. ASME J. Eng. Mater. Technol., 1995, Vol. 117, pp. 330-335.

[30] Y. Takahashi, K. Inoue and K. Nishigushi: Acta Metall., 1993, Vol. 41, pp. 3077-3084.

[31] B. Derby and E. R. Wallach: Met. Sci., 1982, Vol. 16, pp. 49-56.

[32] C. L. Cline: Welding Journal Research Supplement., 1966, pp. 481-489.

[33] J. M. Parks: Weld.J., 1953, Vol. 32(5), pp. 209-221.

[34] W. H. King and W. A. Owczarski: Weld J., 1967, Vol. 46(7).

[35] G. Garmong, N. E. Paton and A. S. Argon: Metall. Trans, 1975, Vol. 6A, pp. 1269-1279.

[36] B. Derby and E. R. Wallach: Metal Science., 1982, Vol. 16, pp. 49-56.

[37] B. Derby and E. R. Wallach: Metal Science., 1984, Vol. 18, pp. 427-431.

[38] J. Pilling, D. W. Livesey, J. B. Hawkyard and N. Ridley: Metal Science., 1984, Vol. 18, pp. 117-122.

[39] I. W. Chen and A. S. Argon: Acta Metall., 1981, Vol. 29, pp. 1759-1768.

[40] K. Nishigushi and Y. Takahashi: The International Conference on Quality and Reliability in Welding., 1984, Hangzhou, China.

[41] Z. X. Guo and N. Ridley: Mater. Sci. Technol., 1987, Vol. 3, pp. 945-953.

[42] A. Hill and E. R. Wallach: Acta Metall., 1989, Vol. 37(9), 2425-2437.

[43] Y. Takahashi and K. Inoue: Mater. Sci. Technol., 1992, Vol. 8, pp. 953-964.

[44] Y. Takahashi and M. Tanimoto: J. Eng. Mater. Technol., 1995, Vol. 117(3), pp. 336-340.

[45] Y. Maehara and T. G. Langdon: Mater. Sci. Eng., 1990, Vol. 128, pp. 1-13.

[46] C. H. Hamilton: Titanium Science and Technology., 1973, pp. 621-647. ed. R. T. Jaffee and H. M. Burke, Plenum Press, New York.

[47] J. R. Williamson: Superplastic Forming of Structural Alloys., 1982, pp. 291-306.

ed. N. E. Paton and C. H. Hamilton, TMS-AIME, Warrendale, PA.

[48] E. D. Weisert and G. W. Stacher: Superplastic Forming of Structural Alloys., 1982, pp. 273-289. ed. N. E. Paton and C. H. Hamilton, TMS-AIME, Warrendale, PA.

[49] E. D. Weisert: Superplasticity in Aerospace., 1988, pp. 315-330. ed. C. Heikkenen and T. R. Mcnelly, TMS-AIME, Warrendale, PA.

[50] D. V. Dunford and P. G. Partridge: J. Mater. Sci., 1987, Vol. 22, pp. 1790-1798.

[51] D. W. Kum, T. Oyama, J. Wadsworth and O. D. Sherby: J. Mech. Phys. Solids., 1983, Vol. 31, pp. 173-186.

[52] H. G. Salem and A. P. Reynolds: J. Mater. Eng. Perform., 2004, Vol. 13(1), pp. 24-31.

[53] K.K. Zhang: Study on Technology of Isothermal Superplastic Solid State Welding. Ph.D Thesis., 2002, pp. 29-33. (in Chinese)

[54] K.K. Zhang, Y. L. Yang, L. Zhao, C. S. Wang and Y. L. Wang: Transactions of the China Welding Institution,. 2006, Vol. 27, pp. 37-40. (in Chinese)

[55] K.K. Zhang, Y. L. Yang and C. S. Wang et al: J. Mater. Sci. Technol., 2001, Vol. 17, pp. 189-190.

[56] K.K. Zhang, H. X. Shi, H. Yu and Y. L. Yang: Transactions of the China Welding Institution., 2008, Vol. 29, pp. 93-97. (in Chinese)

[57] K. K. Zhang Z. L. Zhang S. Liu, et al: China welding,. 2009, Vol. 18, pp. 32-36.

[58] K.K. Zhang, C. X. Han and S. L. Quan et al: Trans. Nonferrous. Met. Soc. China., 2005, Vol. 15(2), pp. 384-388.

[59] H. Kokawa, T. Tsuzuki and T. Kuwara: ISIJ int, 1995, Vol. 35, pp. 1291-1297.

[60] K. K. Zhang , J. Sun, and Z. W. Wu et al: Transactions of the China Welding Institution., 2011, Vol. 32.

[61] Zhang KK 2011 The National Natural Science Funding Project Concluding Report-Grant No.50774029 (Beijing: National Natural Science Foundation of China)

[62] Z. H. Heng, K. K. Zhang and Q. Shuang et al: Electric Welding Machine., 2012, Vol. 42(2), pp. 49-53. (in Chinese)

[63] Z. H. Heng, K. K. Zhang and R. F. Qiu et al: Welding Technology., 2012, Vol. 41(10), pp. 17-20. (in Chinese)

[64] K.K. Zhang, Z.H. Heng, R.F. Qiu, H.X. Shi and Y. Takahashi: IOP Conf. Series: Mater. Sci. Eng., Doc.No. 61(2014) 012002

Chapter 2: Theories

For solid state bonding, the bonding process can be considered as a plastic deformation that occurs at high temperatures for interfacial contact and voids closure. Various kinds of deformation that occur at bonding interface also have an influence on the bonding mechanism. Therefore, to investigate the bonding process, the high temperature deformation and the predominant bonding mechanism should be clarify primarily. Base on the understanding above, the identification method is used to describe bonding process of superplastic materials. In this chapter, the theories of creep deformation, bonding mechanisms, and the identification model will be explained in detail.

2.1 Mechanisms of High Temperature Deformation

Creep is the continuing plastic deformation process that occurs in solids at high temperatures (above approximately $0.5T_m$, T_m is the absolute melting point of the solid) [1], the plastic flow is controlled by three independent mechanisms that can occur at the atomic level. These fundamental mechanisms are migration of dislocation, sliding along grain boundaries, and diffusion of vacancies [1, 2]. They are all thermally activated and are controlled by diffusion of atoms. Therefore, they are temperature- and time-dependent.

Some constitutive equations were developed to elucidate each of above mechanisms. As mentioned in Chapter 1, considering the grain size dependence, the flow stress, σ, can be described as a function of strain rate $\dot{\varepsilon}$ and temperature T, in the following expression:

$$\dot{\varepsilon} = A' \frac{DGb}{kT} \left(\frac{b}{d}\right)^p \left(\frac{\sigma}{G}\right)^n \quad , \tag{2-1}$$

where n is the stress exponent (and is equal to $1/m$, where m is the strain rate sensitivity exponent), and p and A are constants. Each steady state creep deformation can be described by equation (2-1) and has specific values of n, and Q by which the mechanism is identify uniquely.

2.1.1 Diffusional Creep (n = 1)

If the high temperature deformation is a result of the matter transport by diffusion, rather than dislocation movement, the diffusional creep is created. The diffusional creep (Newtonian viscous creep deformation), which exhibits n = 1 at a very high temperature where atom diffusion is rapid. It can be divided into Nabarro-Herring creep (diffusion through the grain lattice) and Coble creep (diffusion through the grain boundary) [3, 4]. Also, the activation energy Q for grain-boundary diffusion is smaller than that for lattice diffusion [2].

2.1.2 Superplastic Creep (n = 2)

Superplastic creep in FSS materials is a plastic deformation controlled by grain boundary sliding. It is characterized by $n = 2$ ($m = 0.5$) and an activation energy which is either equal to the activation energy for grain boundary diffusion Q_b [2, 5-6]. The most commonly considered mechanisms for superplastic deformation involve grain boundary sliding (GBS), and it is necessary for an accommodation process to accompany GBS. The accommodation process might be grain boundary migration, recrystallization, diffusion flow, and some dislocation slip process [2]. Referring to Gifkin's core and mantle model (Fig. 2.1) [7], plastic flow can be considered as arising from two independent processes. In one process, GBS accommodated by slip occurs in the mantle region, and in the other, slip occurs within the core of each grain. When GBS process dominates deformation, superplastic creep can occur, and when the latter process is dominant, the normal creep, which will be explained subsequently, is expected [1, 2, 7].

2.1.3 Dislocation Creep (n = 3-10)

At high stresses (relative to the shear modulus), creep is controlled by the movement of dislocation. It has a strong dependence on the applied stress and no grain size dependence. This dependence is expressed by an equation of the form

$$\dot{\varepsilon} \propto \left(\frac{\sigma}{G}\right)^n, \tag{2-2}$$

in this high temperature regime, n has a value between 3 and 10, then (because of this)

the regime is called dislocation creep. In certain alloys, creep is controlled by the glide alone because solute atoms impede dislocation motion. This leads to a behavior which resembles power law creep with n = 3. This group of materials, in which deformation is controlled by glide of dislocation can also have relatively large elongation [2, 8-9]. Dislocation can acquire a new degree of freedom at high temperature. When the deformation is controlled by the climb of dislocation, the power law creep is established with n=4-6. The limb is generally lattice- diffusion controlled, and hence the activation energy is close to that of volume self-diffusion, Q_v. the rate of power law creep are particularly noted to be independent of grain size [2, 10].

A summary of these various creep mechanisms and their characteristic value are listed in **Table 2.1**.

Table 2.1 High temperature deformation mechanisms.

Creep mode	Mechanism	n	Q
Nabarro-Herring creep	Vacancy Diffusion Through the Grain Lattice	1	Q_v
Coble creep	Vacancy Diffusion Along the Grain Boundary	1	Q_b
Superplastic Flow	Grain Boundary Sliding	2	Q_b
Glide-controlled creep	Controlled by Glide step in Glide/Climb Mechanism	3	Q_v
Power law creep	Controlled by Climb of Dislocation in Glide/Climb Mechanism	4-6	Q_v

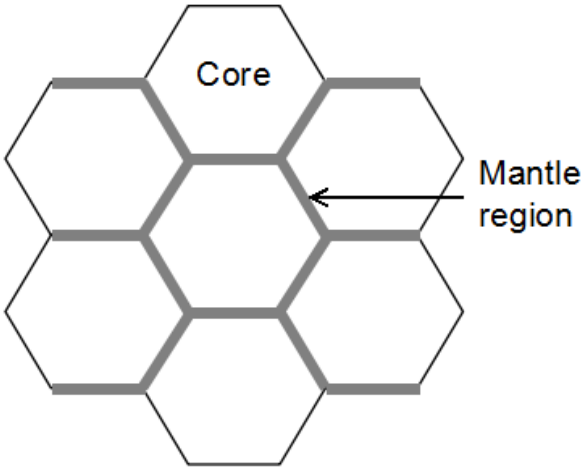

Fig. 2.1 Mantle-like region in superplastic materials.

2.2 Bonding Mechanisms

The processes of solid state bonding can be classified into three stages. During the first stage, the asperities on both bonding surfaces deform plastically as the bonding pressure is applied initially. As the instantaneous plastic deformation proceeds, more metal-to-metal contact is established because of local disruption of the relatively brittle oxide films. The instantaneous plastic deformation proceeds until the localized effective stress at the contact area becomes less than the yield strength of materials at the bonding temperature. The bonded area by instantaneous plastic deformation is less than 10%-20% and a large volume of voids still remain between localized bonded regions at the end of the first stage (the initial stage of solid state bonding) [11, 12].

Subsequently, thermally active mechanisms further lead to void shrinkage and it is assumed that these mechanisms occur independently [13]. The closure of the interfacial voids can occur by three distinct process: (a) interfacial contact by time-dependent plastic deformation (power law creep/or superplastic flow); (b) diffusion of atoms from

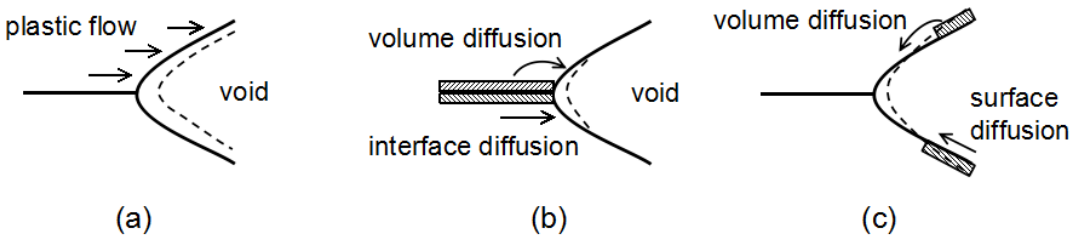

Fig. 2.2 Schematic illustration of mass transfer for void shrinkage. (a) Interfacial contact by time-dependent plastic deformation, (b) Mass transfer from the bonding interface to the void surface, and (c) Surface diffusion from one region of the void surface to another.

the bonding interface to the void surface via both volume and interfacial path; (c) surface diffusion from one region of the void surface to another. These process are illustrated in Fig. 2.2 [14].

The interfacial contact results from the lateral expansion of the supporting material into the void due to the bonding stress (Fig. 2.2 (a)). The plastic deformation contributes to the interfacial contact might be power law creep or superplastic flow (just in FFS materials). The bonding process by plastic flow is restricted as the bonding ratio increases to about 70% and the second (middle) stage of solid state bonding is completed. The diffusional mechanism arise as a consequence of the chemical potential gradient between the stress interface and the surface (stress-free) of the void. Diffusional creep leads to the void shrinkage further until a sound bond is achieved at the third (final) stage of bonding.

It's important to note, however, that only the process (a) and (b) shown in Fig. 2.2 actually reduce the volume of the voids. For diffusional mechanisms, the diffusion flow around the surface of the void (surface diffusion) does not in itself give rise to any

reduction in void volume, otherwise it just changes the void shape [14].

It is also pointed out by Takahashi that interface (grain boundary) diffusion and surface diffusion occur in series, and the surface diffusion step can be ignored because the coefficient of surface self-diffusion D_s is much greater than that of boundary self-diffusion D_b [13].

The summary of bonding mechanisms of solid state bonding during different stages is shown in Fig. 2.3. For FFS materials, after the initial contact by instantaneous plastic deformation is established, the contact process is controlled by high temperature deformation. The plastic flow might be power law creep and also superplastic flow just in case the prerequisite conditions of stress, strain rate, and temperature are obtained. In the final stage, the diffusional mechanisms such as interface self-diffusion and volume self-diffusion dominate the bonding process. In the present study, the predominant bonding mechanisms of solid state bonding of FFS materials will be investigated by the identification model introduced in next section.

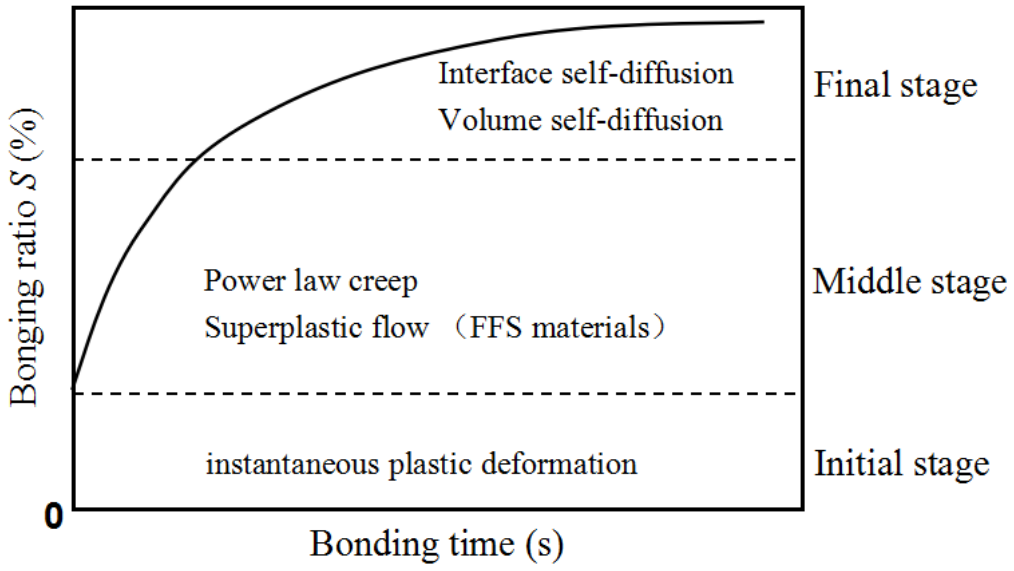

Fig. 2.3 Bonding mechanisms of solid state bonding.

2.3 Identification of Predominant Bonding Mechanisms

Based on the existing models of diffusion bonding [12, 13], the void shrinkage mechanisms can be comprehended under any particular conditions. The models can also be verified well by the calculation results and the experimental results. Referring to the identification model proposed by Takahashi [12], the fundamental void shrinkage mechanisms can be distinguished from experimental date with respect to percentage bonded area (bonding ratio). In the present study, a modified model with triangular interfacial voids is proposed to identify the predominant bonding mechanisms including superplastic deformation for the particular FFS materials [15-17].

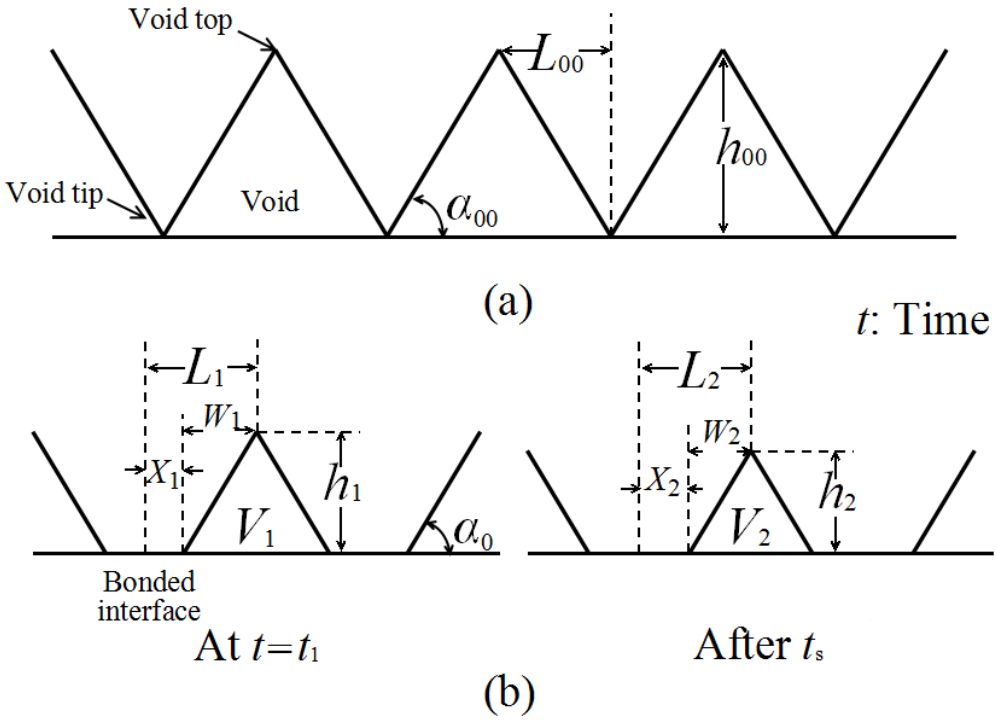

Fig. 2.4 Schematic illustrations for voids on the bonding interface. (a) Cross section of the voids arranged in regular intervals before bonding. (b) Representation of void shrinkage from V_1 to V_2 in the period of t_s.

To simplify the calculation, the cross section of the voids is assumed to be triangular. In other words, the bonding surface of superplastic material with high deformability is machined to regular ridges (parallel or circular) and that of non-superplastic hard material is assumed to be perfectly flat and changeless.

Fig. 2.4 schematically illustrates the cross section of bonding interface during bonding. Fig. 2.4 (a) shows the initial contact before the instantaneous plastic deformation. The triangular void (interval of $2L_{00}$) is used to analyze the void shrinkage during the bonding. If bonding process occurs in the conditions of high temperature and high vacuum between similar materials, the influences of inter-diffusion and oxide film can be ignored [11].

The voids shrinkage ΔV (= V_2-V_1) in the period of t_s (= t_2-t_1) is shown in Fig. 2.4 (b). The geometrical parameters X, w, and h in Fig. 2.4 are, respectively, half of the bonded length of a unit, half the void width, and the void height. The dihedral angle of initial void shape before bonding is α_{00} and that of void shape during bonding at $t = t_1$ is α_0. The angle α_0 is different from α_{00} because the instantaneous plastic deformation is produced. The angle of void shape can also change during bonding by the plastic flow. If the volume of ΔV is small enough, the dihedral angle can be assumed constant.

Here, it is noted that the flat bonding surface of non-superplastic material can also deform more or less under the bonding stress and high temperature. But interfacial deformation mainly occurs on the side of the superplastic metal under identical bonding conditions, that is, the plastic deformation of the non-superplastic metal need not be considered.

In general, the instantaneous plastic deformation operates in the bonding ratio less than 20% during the initial bonding stage. In the present study, the set value X_1 is greater

than the critical value X_c given by the instantaneous plastic flow, thus, the contribution of instantaneous plastic deformation to the interfacial contact can be ruled out [15-17]. Referring to the identification model proposed by Takahashi [12], the relation between bonded area growth ΔX and time t_s is expressed by

$$\Delta X = \frac{A_c}{kT} \cdot \left(\frac{P}{G}\right)^n \exp\left(-\frac{Q}{RT}\right) \cdot M\{F(L, X, n)\} \cdot t_s, \tag{2-3}$$

where n is the stress exponent, A_c is a constant, P is the bonding pressure, G is the shear modulus, F (L, X, n) is a geometrical function of L, X, and n, Q is the activation energy for creep deformation. t_s is the time required to obtain a certain void shrinkage ΔV (bonding ratio increment ΔS), ΔV is roughly proportional to the bonded area increment ΔX. If ΔX is kept constant, M {F (L, X, n)} also becomes constant, t_s can be estimated by ΔX whichever mechanism is predominant. The following relations are expressed as

$$t_s \propto \left(1/P\right)^n \tag{2-4}$$

and if G is assumed to be constant against temperature change,

$$\frac{T}{t_s} \propto \exp\left(-\frac{Q}{RT}\right) \tag{2-5}$$

is established. T should be designated properly and kept constant and P should be kept constant during the bonding process. So, the predominant mechanism during solid state bonding can be identified by the gradients of log t_s vs log P and log (T/t_s) vs (1/T) plots, that is, the gradients are the stress exponent, n, and the activation energy, Q, respectively. According to the characteristic values of high temperature deformation mechanisms,

the predominant bonding mechanisms can be distinguished from each other.

For instance, the n value is about 4~6 when power law creep is predominant, whereas the n value is about 2~3 and the Q value is close to the interface self-diffusion activation energy Q_b, in the case of that the superplastic flow is predominant during solid state bonding. The prediction of predominant bonding mechanism identified by the modified model is shown in Table 2.2.

Table 2.2 A summary of predominant bonding mechanisms

Bonding mechanism	Stress exponent n	Activation energy Q
Instantaneous plastic deformation	-	-
Interface self-diffusion	~1	Q_b
Volume self-diffusion	~1	Q_v
Superplastic Flow	2~3	Q_b
Power law creep	4-6	Q_v

References

[1] A. K. Mukherjee: High Temperature Creep., 1975, Academic Press, New York, pp. 163-170.

[2] T. G. Nieh: Superplasticity in Metals and Ceramics., 1997, Cambridge University Press, New York.

[3] F. R. N. Nabarro: Phil. Mag. A., 1967, Vol. 16, pp. 231-237.

[4] C. Herring: J. Appl. Phys., 1951, Vol. 21, pp. 437-445.

[5] S. Hori, M. Tokizane and N. Furushiro: Superplasticity in Advanced Materials., 1991, Osaka, Japan.

[6] T. G. Langdon: Metall. Trans., 1982, Vol. 13, pp. 689-701.

[7] RC. Gifkins: Metall Trans., 1976, Vol. 7, pp. 1225.

[8] O. D. Sherby and P. M. Burke: Porg. Mater. Sci., 1967, Vol. 13, pp. 325-390.

[9] J. Weertman: J. Appl. Phys., 1957, Vol. 28, pp. 1185-1191.

[10] J. Weertman: Trans. ASM., 1968, Vol. 61, pp. 681-694.

[11] Y. Takahashi: Ceramic Trans., 2003, Vol. 138, pp. 29-47.

[12] Y. Takahashi, K. Inoue and K. Nishigushi: Acta Metall., 1993, Vol. 41, pp. 3077-3084.

[13] Y. Takahashi and K. Inoue: Mater. Sci. Technol., 1992, Vol. 8, pp. 953-964.

[14] J. Pilling: Mater. Sci. Eng., 1988, Vol. 100, pp. 137-144.

[15] Z.H. Heng, M. Maeda and Y. Takahashi: IOP Conf. Series: Mater. Sci. Eng., Doc.No. 61(2014)012003.

[16] Z.H. Heng, T. Matsushima, Y. Nashiki, M. Maeda, K.K. Zhang and Y. Takahashi: Quarterly Journal of the Japan Welding Society., 2015, Vol. 33(2), pp. 67-70.

[17] Z.H. Heng, T. Matsushima, Y. Nashiki, M. Maeda and Y. Takahashi: Journal of Smart Processing., 2015, Vol. 4, pp. 102-108.

Chapter 3: Experimental Procedure

To investigate the solid state bonding of superplastic materials in the present study, the preparation of superplasticity is indispensable. Superplasticity depends on two prerequisites. The first is the material conditions such as chemical components, and microstructure (grain size, grain shape, and distribution). Secondly, the conditions of superplastic deformation including deformation temperature, and strain rate should also be appropriate [1-4]. Base on the heat treatment for superplasticity, mechanical characteristics of superplastic steel being bonded are verified by the compression test to determine the bonding conditions. The superplastic steels with different surface asperities are prepared and then for the solid-state bonding in the superplastic range of temperatures and stresses. The analysis of bonding process and microstructure after bonding are also introduced in this chapter.

3.1 Preparation of Specimens

Fine-structure superplasticity (FSS) requires a stable microstructure with fine, and equiaxed grain. Dual phase steel can show superplasticity after the heat treatment for refining microstructure [2, 5].

As shown in the shadow areas of Fig. 3.1, hypoeutectoid steels with the structure of ferrite and austenite (the ratios are similar) can exhibit superplasticity well. Superplasticity can also be readily achieved in eutectoid and hypereutectoid steels due

to the evenly distributed carbides. The superplasticity increases with the rising of carbon content. The superplastic range of temperatures for carbon steels is close to the A_1 temperature (Lower critical temperature) and the strain rate is usually in the range of $10^{-2}s^{-1}$ to $10^{-5}s^{-1}$ [2, 5-7]. In the present study, high carbon steel SK105 was adopted to produce superplastic steel.

3.1.1 Heat Treatment

The chemical components of SK105 are similar with that of tool steel T10A as show in Table 3.1 [8, 9]. Superplasticity in this kind of high carbon steel can be produced. The original steel with its coarse pearlite structure (grain size ＞ 10μm) shown in Fig. 3.2 cannot exhibit superplasticity behavior. The heat treatment of cyclic phase transformation was used to refine microstructure. The process which refers to the treatment of T10A [5, 8-9] is shown in Fig. 3.3. After circular quenching from 1053K three times, followed by tempering at 473K, fine tempered martensite (grain size: 5~8μm) shown in Fig. 3.4 was obtained. The superplastic steel SK105 for solid state bonding in the present study is produced [10, 11].

Table 3.1 Chemical components of SK105 and T10A.

Steel	Chemical components				
	C	Cr	Mn	Si	Ni
SK105	0.92	0.18	0.64	0.28	0.09
T10A	0.95~1.04	≤ 0.25	≤ 0.40	≤ 0.35	≤ 0.12

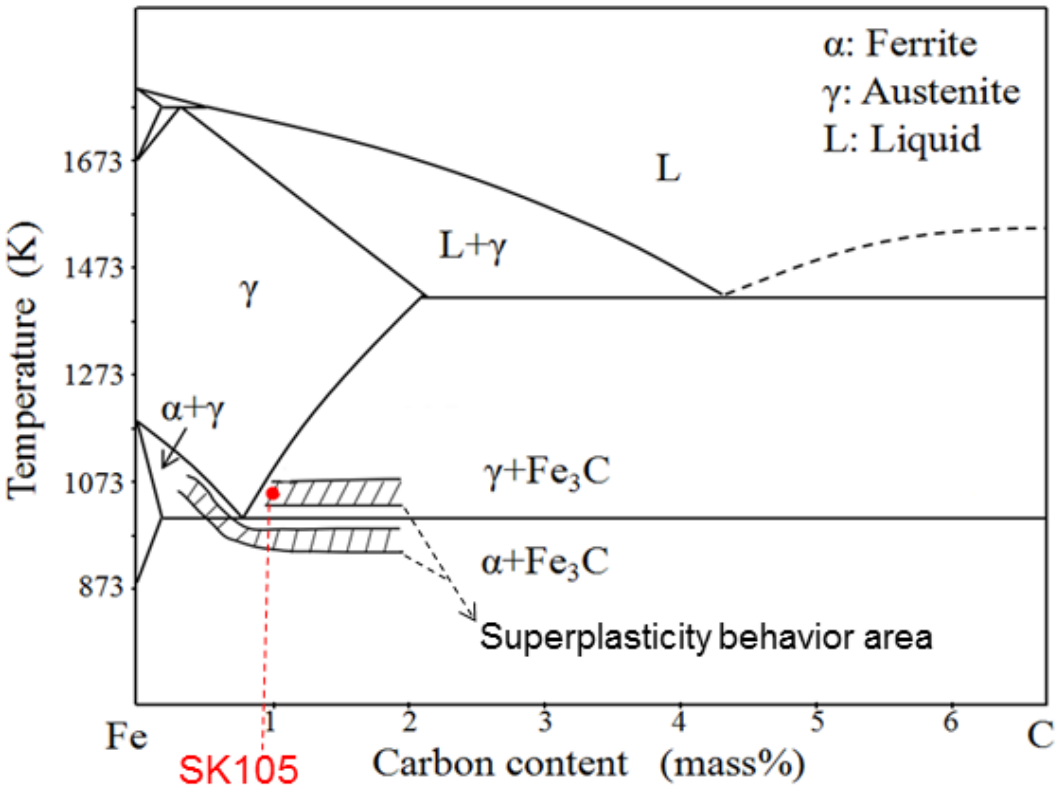

Fig. 3.1 Superplastic region of dual phase steel in Fe-C phase diagram.

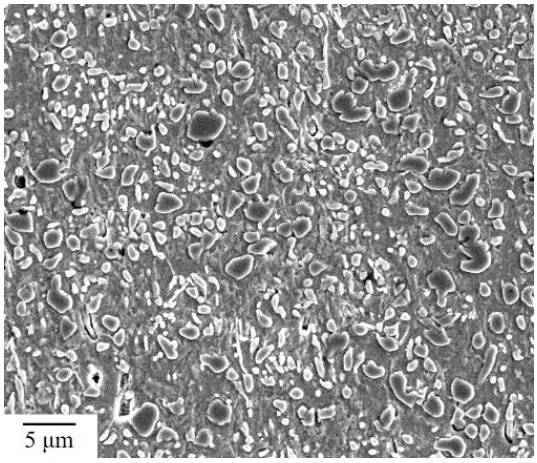

(a) Pearlite in original steel

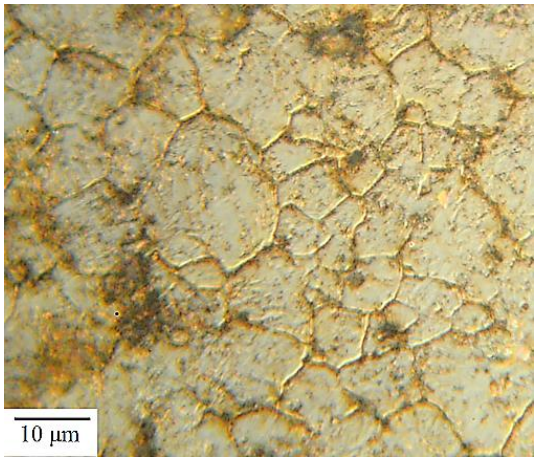

(b) Grain size of original steel

Fig. 3.2 Microstructure of original steel SK105.

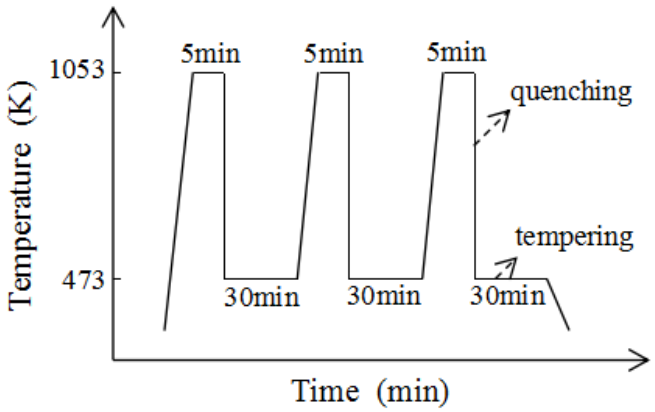

Fig. 3.3 Heat treatment process of superplastic SK105.

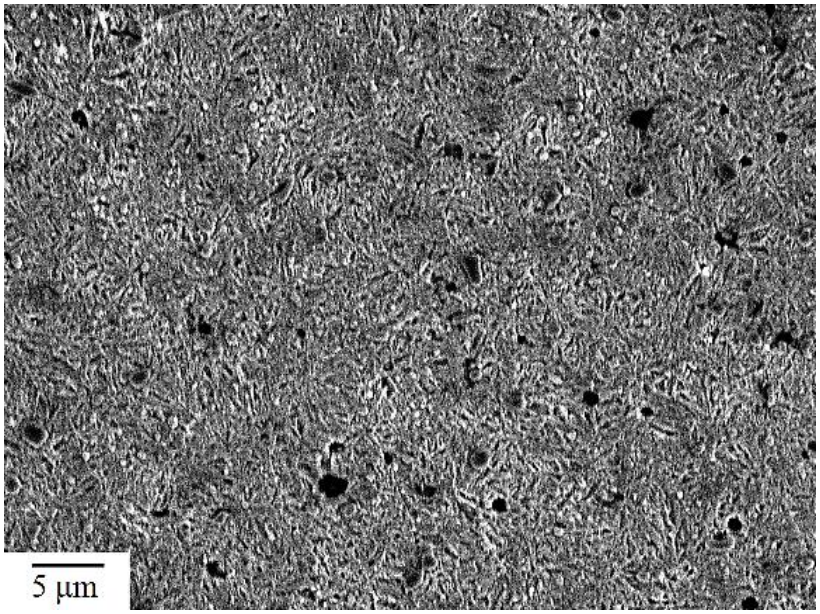

(a)

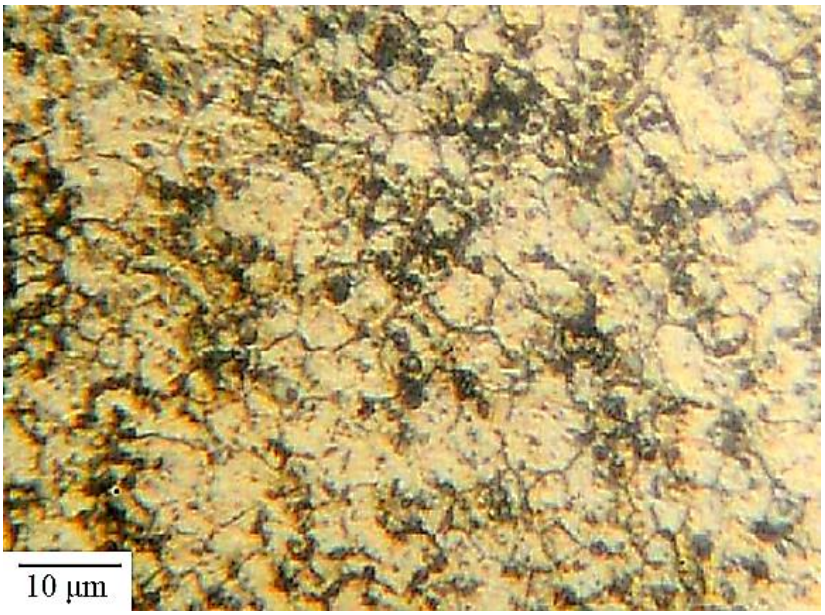

(b)

Fig. 3.4 Microstructure of superplastic steel SK105. (a) Tempered martensite in superplastic steel, and (b) Grain size of superplastic steel.

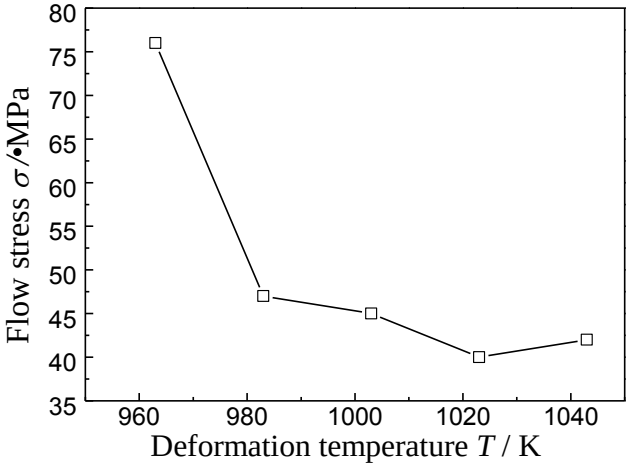

(a)

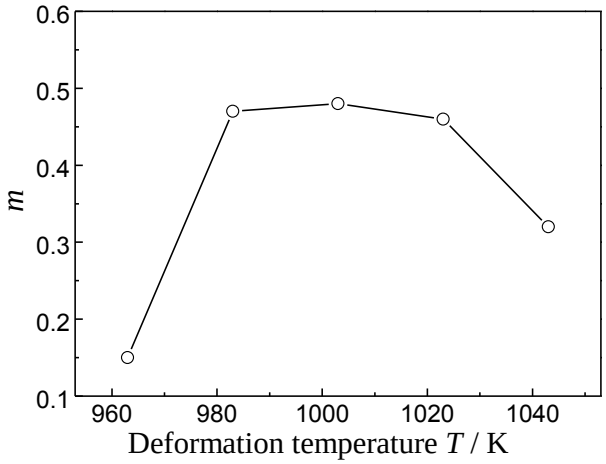

(b)

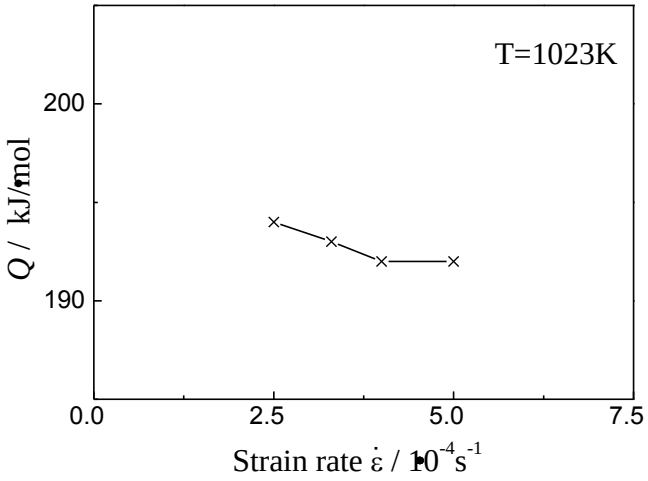

(c)

Fig. 3.5 Compression test of superplastic steel T10A.

Table 3.2 Mechanical characteristics of superplastic steel T10A.

Test	Mechanical Characteristics of superplastic steel T10A				
	Superplastic temperatures T / K	Strain rate $\dot{\varepsilon}\times10^{-4}s^{-1}$	σ/MPa	m	Q/kJ mol^{-1}
Tension	923,1023-1043	1.7-2.0	-	0.35	-
Compression	1003-1043	2.5-5.0	35-45	0.32-0.48	183-194

3.1.2 Mechanical Characteristic

The mechanical characteristics of superplastic steel SK105 including the flow stress σ, m, and Q, should be investigated to set the bonding parameters before the solid state bonding. So far the superplastic parameters of materials are usually obtained by the tensile test. However, solid state bonding is essentially based on the interfacial compression deformation. Therefore, it is necessary to estimate the mechanical characteristics of SK105 during the superplastic deformation.

Due to the conformity of chemical components and microstructure, the superplastic behaviors of SK105 can be comprehended by the compression test of T10A [8, 9] as shown in Fig. 3.5 and Table 3.2.

Likewise, it can be inferred that the fine grained high carbon steel SK104 can show superplasticity under conditions of superplasticity-causing temperatures (T = 1003~1043K) and flow stresses (σ = 35~45MPa). The value of m is larger than 0.3 and the activation energy, Q, is about 194 kJ mol^{-1} which is close to the activation energy of γ-Fe interface (grain boundary) self-diffusion, Q_b.

3.1.3 Bonding Surfaces

Bonding specimens SK104 used in the present study are cylindrical and the size is Φ10mm×12mm.

Generally, the actual bonding process controlled by visco-plastic deformation mechanisms can be influenced by the geometrical factor: initial void shape with the surface asperity angle α_{00}, which is defined as

$$\alpha_{00} = \tan^{-1}(h_{00}/L_{00}), \tag{3-1}$$

where h_{00} is the surface asperity height and L_{00} is half the surface asperity length as shown in Fig. 2.4(a) before bonding. The initial void shape is changed by the angle α_{00}. The interfacial contacting mode which controls the rate of void shrinkage can be changed by the angle α_{00} and initial void shape [12-14].

In the present study, superplastic steels with three types of bonding surfaces (as shown in Table 3.3 and Fig. 3.6) were prepared for the bonding tests.

Specimen 1 and Specimen 2 with relatively coarse and regular bonding surfaces were adopted to investigate the bonding process controlled by dislocation creep deformation. Moreover, Specimen 3 with fine bonding surface was for investigating the bonding process controlled by diffusional mechanisms. The bonding surface of specimen 3 is not uniform due to the abrasive paper-making. The estimated values of L_{00} and h_{00} are therefore adopted.

It is difficult to make the voids more sharp (α_{00} > 50 deg) or to make the ridges more fine due to the hardness of high carbon steel. These three types of bonding surfaces of superplastic SK104 were adopted to identify the predominant bonding mechanisms,

thus analyzing the influence of surface roughness on the interfacial contacting process. As mentioned in Section 2.3, the bonding surface of original steel without superplasticity was machined to be perfectly flat.

Table 3.3 Bonding specimens of superplastic steel.

Specimen	L_{00} /μm	h_{00} /μm	α_{00} /deg	Surface description	Machining method
1	80	30	20	Concentric circular ridges	Lath-machined
2	500	500	45	Parallel line ridges	Wire cutting
3	8-15	1.5-4	-	One direction ridges	Abrasive paper

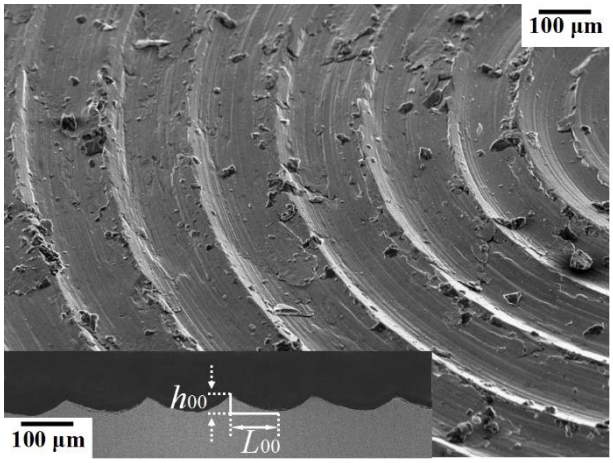

(a)

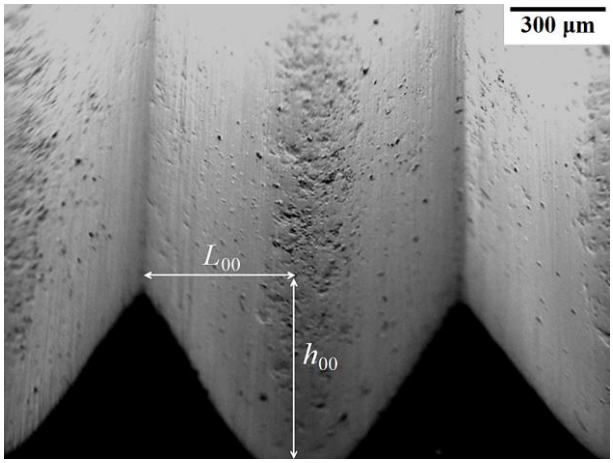

(b)

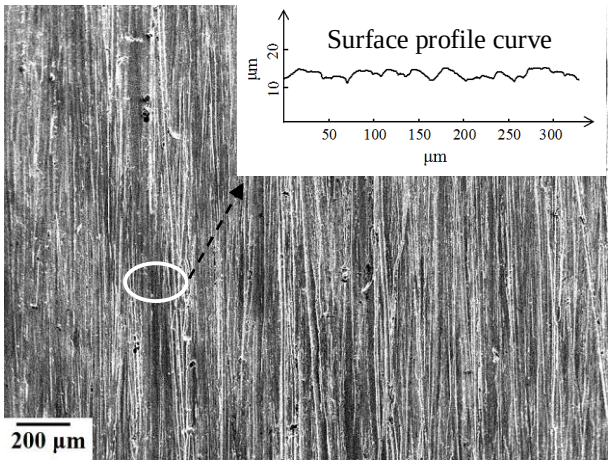

(c)

Fig. 3.6 Appearances of bonding surfaces of superplastic SK104. (a) Specimen 1 with slightly coarse surface and its cross sectional view, (b) Specimen 2 with coarse surface, (c) Specimen 3 with fine surface and its surface profile curve.

3.2 Bonding Apparatus and Bonding Conditions

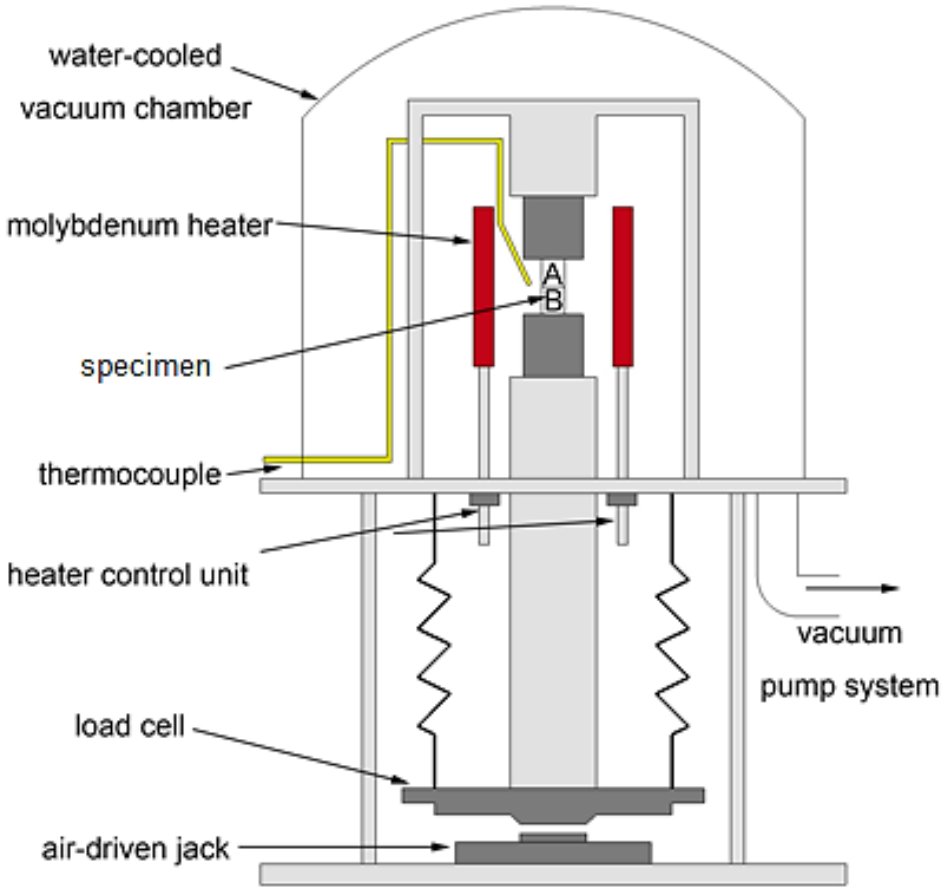

Fig. 3.7 Schematic illustration of bonding apparatus.

Table 3.4 Couple of bonding specimens.

Specimen	Steel	Bonding surfaces
A	Superplastic (shown in Fig. 3.6)	Specimen 1 slightly coarse Specimen 2 coarse Specimen 3 fine
B	Original (without FSS)	Mirror surfaces

In order to rule out the influence of high-temperature oxidation, the bonding tests were carried out in vacuum (atmospheric pressure is 10^{-4} Pa). The pressure was applied in the form of a uniaxial compressive stress. The bonding apparatus is shown in Fig. 3.7. The couple of bonding specimens as shown in Table 3.4 were heated using a molybdenum heater and cooled after the bonding pressure was removed. There is no constraint stress applied to the specimens during heating process due to the balance control of lower pressing head. Therefore, the bonding time is the period when the bonding pressure is applied [10-12].

Referring to the mechanical characteristics of SK105 during superplastic compression, the bonding tests between superplastic steel and original steel were carried out under several conditions for estimating the time t_s required to attain a certain bonding ratio increment ΔS. The bonding temperature was in the range of SK105 superplastic temperatures (1003~1053K). The range of bonding pressure was 15~60MPa.

3.3 Analysis of Bonding Process

3.3.1 Bonding Surfaces

The bonding ratio S and the void shrinkage ΔV can be measured by the scanning electron microscope (SEM) observation of the fracture surfaces and cross section views (Specimen A in Fig. 3.8) after bonding. As shown, the bonding joints were pretreated in liquid nitrogen for several minutes to avoid the interfacial plastic deformation during breaking, thus making the results more accurate.

Choosing an appropriate ΔS is necessary for identifying the predominant mechanisms

in the middle stage of solid state bonding as mentioned in Section 2.3. It takes a long time to obtain a large value, ΔS, when the diffusional mechanisms is predominant under the conditions of low bonding pressure. Conversely, the estimation of bonded area will be inaccurate if the set value of ΔS is relatively small, compared with the voids size. In consideration of the feasibility of bonding test and the reliability of results, the set value of S_1, S_2, and ΔS are shown in Table 3.5.

Three repetitions of bonding tests under each condition were carried out and the mean values were used to ensure the accuracy of ΔS estimation. It is difficult to detect the bonded area or to get the time t_s directly during the bonding. It is assumed that the bonding ratio S is linearly dependent on the time t in a relatively narrow range of bonded area increment. Therefore, t_s can be estimated by interpolating the data of several bonding tests as shown in Fig 3.8, and then the value of n and Q during the bonding process can be figured out by the identification model.

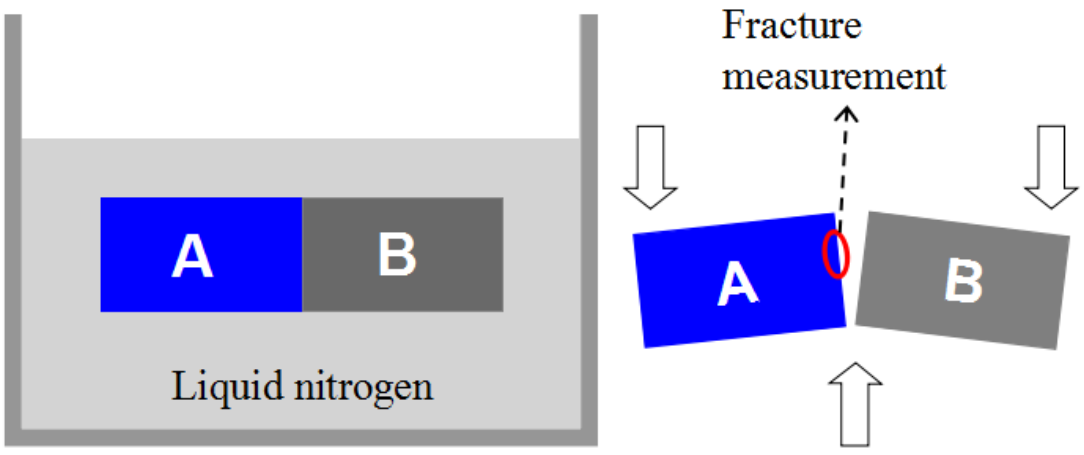

Fig. 3.8 Schematic illustration of fracture observation.

Table 3.5 Pre-setting of bonding process.

Specimen	S_1	S_2	ΔS	Identification
1	30%	50%	20%	Creep flow
2	30%	40%	10%	Creep flow
3	65%	72%	7%	Diffusional

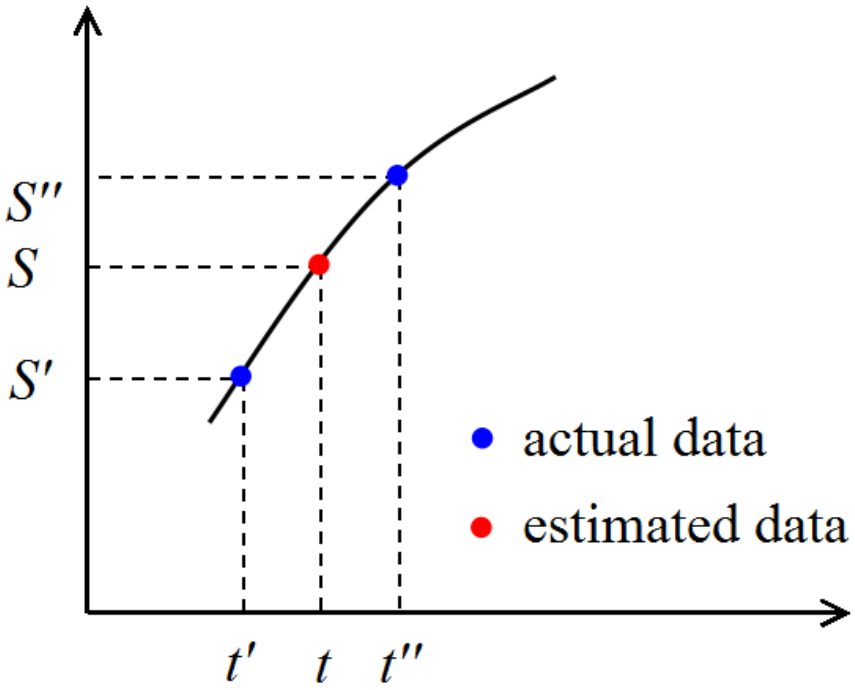

Fig 3.9 Interpolation method for estimating the time t_s.

(t_s is the time required to attain a certain bonding ratio increment ΔS)

3.3.2 Microstructure Observation

The predominant bonding mechanisms can be identified by the characteristic value, *n* and *Q*. In addition, the interfacial deformation controlled by fundamental mechanisms can also be reflected by the interfacial microstructure after bonding. The interfacial microstructure after etching by oversaturated picric acid were observed by SEM or optical microscope. As shown in Fig. 3.10, the shadow area of superplastic steel close to the bonding interface undergo various deformation during bonding process. The microstructure characteristics including the grain size, and the grain shape were observed. If the superplastic flow is dominant, the microstructure with superplastic characters should be remained. In other worlds, there is no obvious grain growth or shape change. However, unlike the superplastic flow, the grain growth can occur along with high temperature deformation when the diffusional mechanism or power law creep is predominant. The equiaxed grains of superplastic steel can also deform along the direction of bonding pressure.

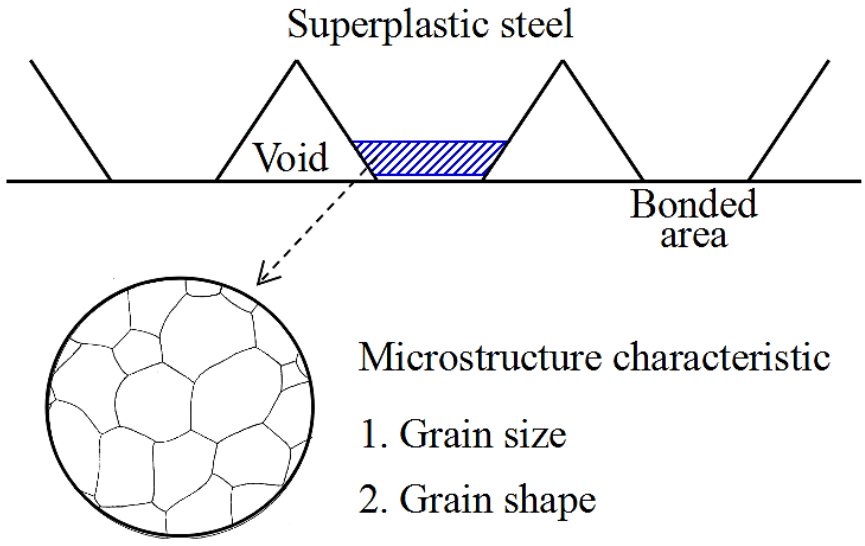

Fig. 3.10 Observation zone of interfacial microstructure.

References

[1] TG. Langdon: 4th International Conference on Superplasticity in Advanced Materials., 1991, Osaka.

[2] TG. Nieh: Superplasticity in Metals and Ceramics., 1997, Cambridge University Press, New York.

[3] Y. Maehara and TG. Langdon: Mater. Sci. Eng., 1990, Vol. 128, pp. 1.

[4] RZ. Valiev: Mater. Sci. Eng., 1997, Vol. 234. Pp. 59-66.

[5] K.K. Zhang, Z.H. Heng, R.F. Qiu, H.X. Shi and Y. Takahashi: IOP Conf. Series: Mater. Sci. Eng., Doc.No. 61(2014) 012002

[6] Z.L. Zhang, Y.L. Liu, J.W. Zhu and G. Yu: Mater. Sci. Eng., 2008, Vol. 64, pp. 483-484.

[7] K.K. Zhang, Y.L. Yang, C.S. Wang, H.K. Li and J. Xue: Mater. Sci. Technol., 2001, Vol. 17, pp. 189.

[8] K.K. Zhang: Study on Technology of Isothermal Superplastic Solid State Welding. Ph.D Thesis., 2002, pp. 29-33. (in Chinese)

[9] Y.L. Yang, K.K. Zhang, C.S. Wang, N. Zhao and X.M. Xu: J. Iron. Steel. Res., 2004, Vol. 16(6), pp. 65-68. (in Chinese)

[10] Z.H. Heng, M. Maeda and Y. Takahashi: IOP Conf. Series: Mater. Sci. Eng., Doc.No. 61(2014)012003.

[11] Z.H. Heng, T. Matsushima, Y. Nashiki, M. Maeda, K.K. Zhang and Y. Takahashi: Quarterly Journal of the Japan Welding Society., 2015, Vol. 33(2), pp. 67-70.

[12] Z.H. Heng, T. Matsushima, Y. Nashiki, M. Maeda and Y. Takahashi: Journal of Smart Processing., 2015, Vol. 4, pp. 102-108.

[13] Y. Takahashi and M.Tanimoto: Trans. ASME J. Eng. Mater. Technol., 1995, Vol. 117, pp. 336-340.

[14] Y. Takahashi and M.Tanimoto: Trans. ASME J. Eng. Mater. Technol., 1995, Vol. 117, pp. 330-335.

Chapter 4: Bonding Process Controlled by High Temperature Deformation

As mentioned before, the initial stage of solid state bonding is produced by instantaneous plastic deformation. Subsequently, various creep deformations lead to the bonding process in the middle bonding stage [1, 2]. In this chapter, the solid state bonding of superplastic steel (Specimen 1 and Specimen 2) with coarse bonding surfaces and original steel is investigated under different bonding conditions. The bonding process controlled by plastic flow can be identified by the characteristic value (n and Q) during bonding and the microstructure after bonding without considering diffusional mechanisms. The effect of bonding surface roughness on interfacial contact process is also discussed. A good understanding of bonding process due to high temperature deformation is described in this chapter.

4.1 Bonding Tests

Creep deformation dominates the bonding process under the conditions of relatively high bonding temperatures and coarse bonding surfaces. Therefore, Specimen 1 and Specimen 2 were adopted to bond with original steel under different bonding pressures and bonding temperatures. The time t_s required to attain a certain bonding ratio increment ΔS was measured, thus figuring out the values of n, and Q. The bonding results are shown as follows.

4.1.1 Bonding Results of Specimen 1

Fig. 4.1 shows the bonding process and surface fractures of Specimen 1 at different bonding stages. The void shrinkage is relatively uniform. The bonded area can be defined by the fracture shape. The rugged and bright areas are the bonded zones; the dark areas are the initial surfaces of voids. When the bonding time t = 0 s, the initial contact, S, is 0%. S_1 = 20% is set as the Stage 1, for a bonding time of t_1. When the bonding time $t_2 = t_1 + t_s$, S_2 = 50% and the bonding ratio increment ΔS is set to 20% at Stage 2.

Fig. 4.2 shows the bonding ratio under different bonding pressures. From the bonding results, the time t_s significantly decreases as the bonding pressure increases. The bonding ratio is linearly proportional to the bonding time t just in the narrow range between two experimental results. The interpolation method can be possible. When the

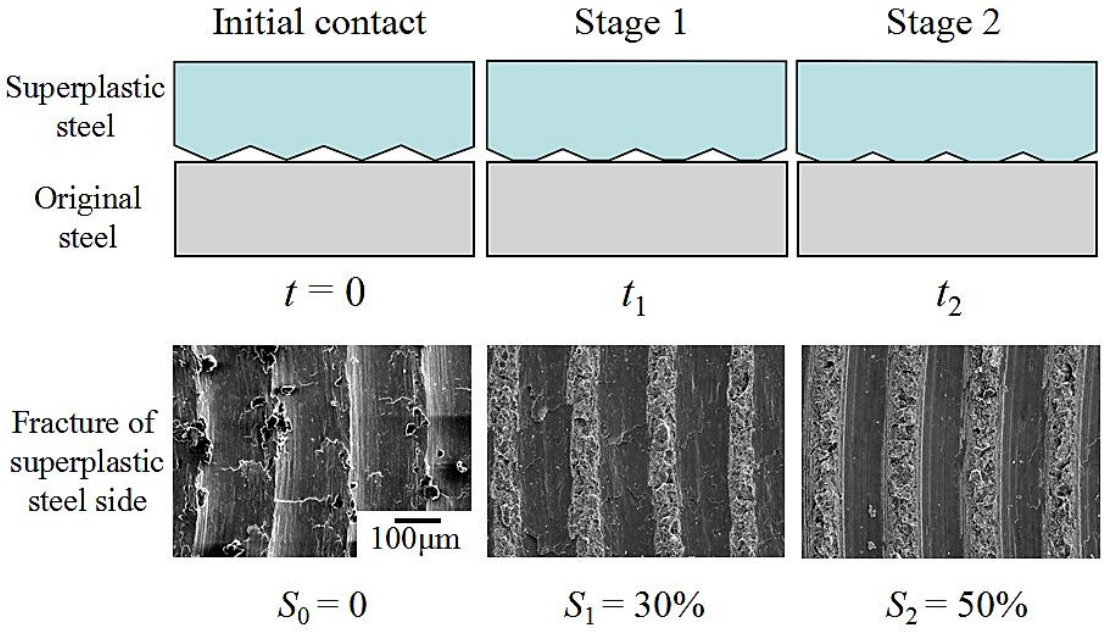

Fig. 4.1 Fractured surfaces of Specimen 1 at different bonding stages.

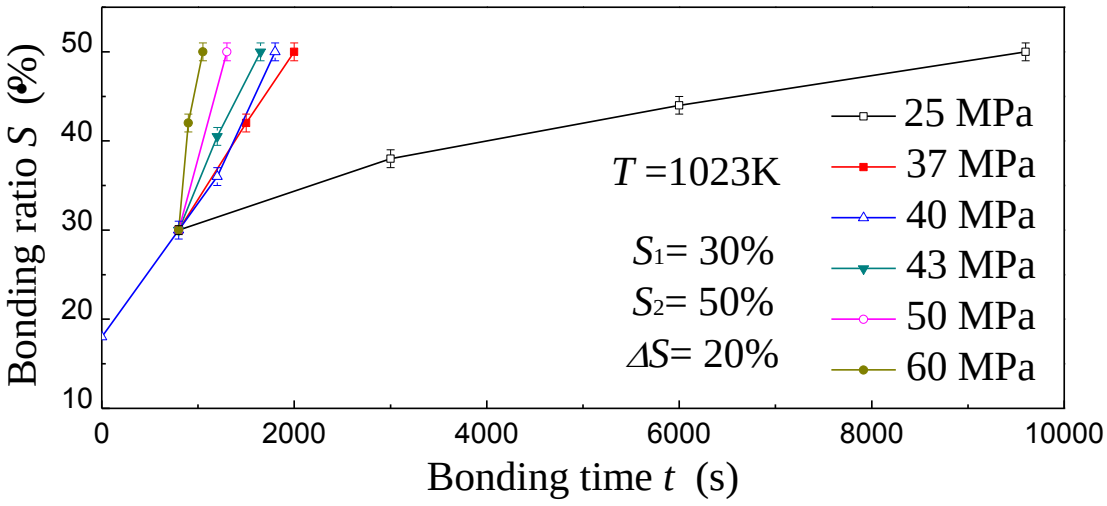

Fig. 4.2 Bonding time dependence of bonding ratio in Specimen 1.

bonding pressure P is 40MPa and the bonding time t_1 is 850s, the bonding ratio S_1 = 30% is set as Stage 1. Subsequently, the bonding process is continued under different bonding pressures. Therefore, assuming there is a linear relation between t and S in a narrow range of ΔS, the bonding time t_2, which is to obtain a certain bonding ratio increment ΔS = 20%, can be calculated by using the interpolation method (shown in Fig. 3.9). The time t_s, which is from Stage 1 to Stage 2, can be figured out. After a series of bonding time t_s are attained, the values of n and Q can be calculated by the identification method introduced in Section 2.3.

4.1.2 Bonding results of Specimen 2

The fractured surfaces of Specimen 2 are shown in Fig. 4.3. Although the void surface machined by wire cutting is relatively coarse, the bonded area can be separated from the void surface clearly. The bonded areas are marked by the blue bars while the void

surfaces are marked by the gray bars. Fig. 4.4 shows the bonding results of Specimen 2 at T = 1023K. Similarly, when P = 35MPa and t = 20 mins, the bonding ratio S_1 = 30% is set as Stage 1. A linear relation between t and S can be also obtained in a narrow

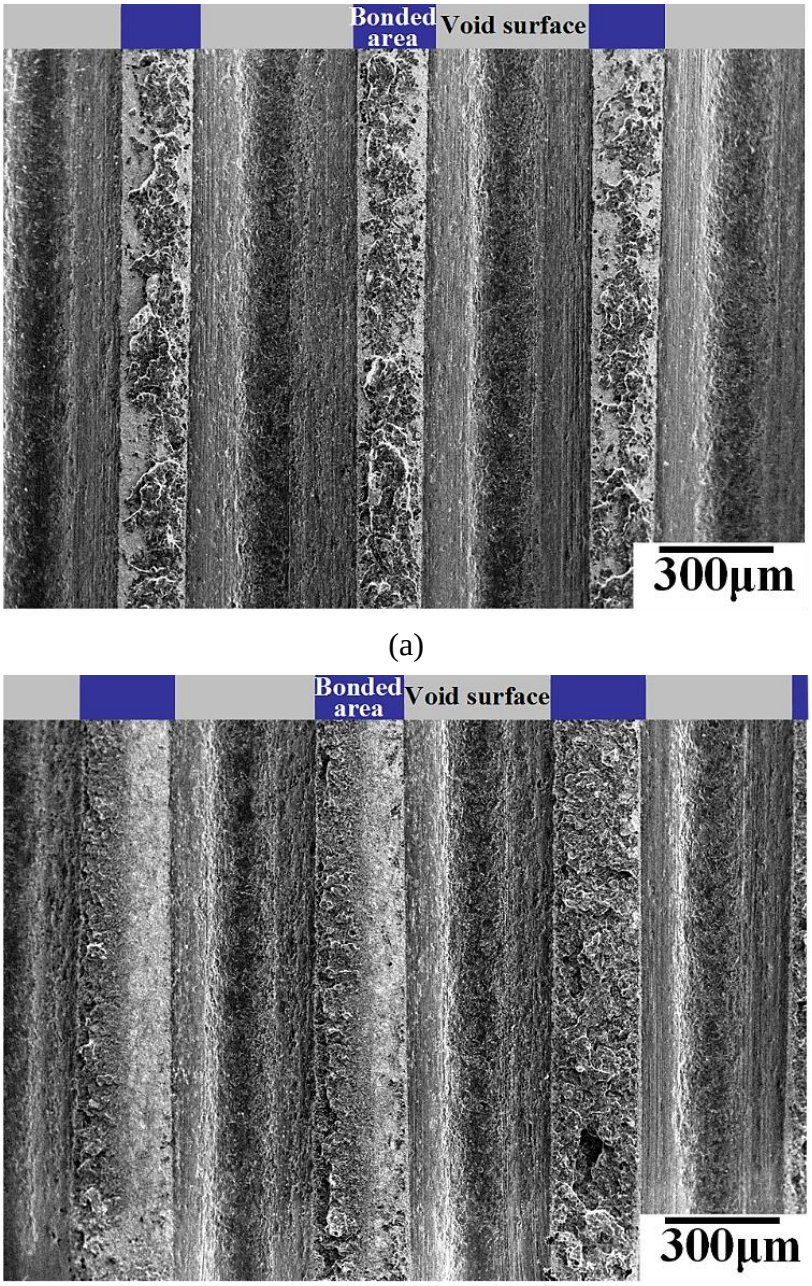

Fig. 4.3 SEM observations of fractured surfaces of Specimen 2.

(a) S_1 = 30%, (b) S_2 = 40% (T = 1023K, P = 40MPa).

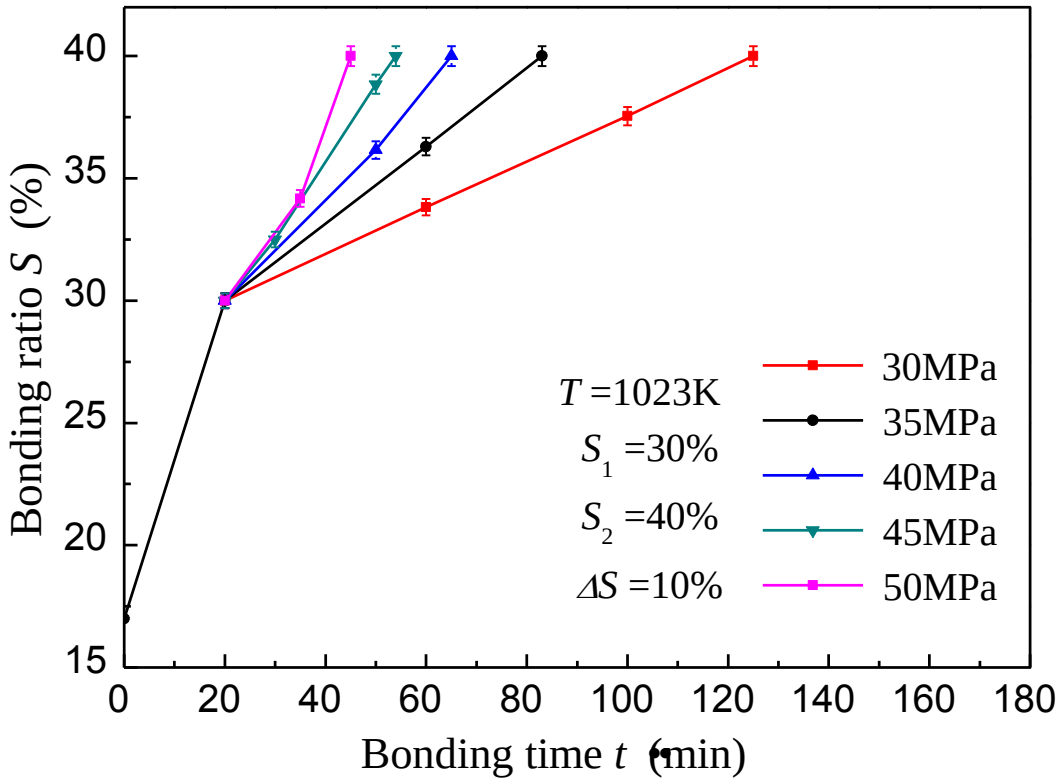

Fig. 4.4 Bonding time dependence of bonding ratio in Specimen 2.

range of ΔS. For Specimen 2, a relatively small bonding ratio increment was adopted due to the large dimension of voids. Therefore, the bonding ratio S_2 = 40% is set as Stage 2. A series of time, t_s, can be estimated under different bonding pressures as well.

4.2 Interfacial Contact Process Controlled by Superplastic Flow

The characteristic value of n and Q during bonding process can be calculated by the time t_s from equations (2-4) and (2-5). The interfacial microstructure after bonding can also indicate the dominant deformation during the bonding process.

4.2.1 Stress Exponent, *n*

Fig 4.5 and Fig 4.6 show the bonding pressure dependence of t_s under the conditions of T = 1023K and different bonding pressures in Specimen 1 and Specimen 2 respectively. For Specimen 1, as shown in Fig 4.5, the value of *n* is different and it changes with the bonding pressure, as a result of a change of the predominant bonding mechanism. The value of *n* is about 2.3 for the bonding pressure P = 37~43MPa. The strain rate sensitivity index, *m* (reciprocal of *n*), is about 0.43. This suggests that superplastic deformation predominantly contributes to the interfacial contact process. In other words, superplastic flow-based deformation occurs at the bonding interface at this stage from a bonding ratio of 30% to 50%.

When the bonding pressure is beyond the range of 37MPa to 43MPa, *n* is large than 3. The superplastic flow can no longer be dominant and the predominant bonding mechanism changes to power law creep, as explained in next section. If the *n* value lies between the specific values associated with these two fundamental mechanisms, a combined effect of these two mechanisms can be expected to occur.

By extending the characteristic curves of the different mechanisms, the intersection point is obtained. This point can be considered as a transition point of these two fundamental mechanisms. Thus, the bonding pressure range can be divided into three regions, as shown in Fig 4.5. When the bonding pressure is in the middle range, P = 34~44.3MPa, the superplastic flow is predominant [3, 4].

Fig 4.6 shows the *n* value of Specimen 2. The changes in *n* value of Specimen 2 are similar to that of Specimen 1. The *n* value is about 2.52 for the bonding pressure P = 35~40MPa. The *m* value is about 0.4. It suggests that the interfacial contact process is

greatly controlled by superplastic deformation. When P = 40~45MPa, the n value is equal to 2.37 and the superplastic flow predominantly contributes to the bonding process. The superplastic range of bonding pressure from 35MPa to 45Mpa, which is basically the same as that of Specimen 1, is obtained. When the n value is close to or more than 3, the combined effects of two or more distinguishable mechanisms act on the interfacial contact process [4, 5].

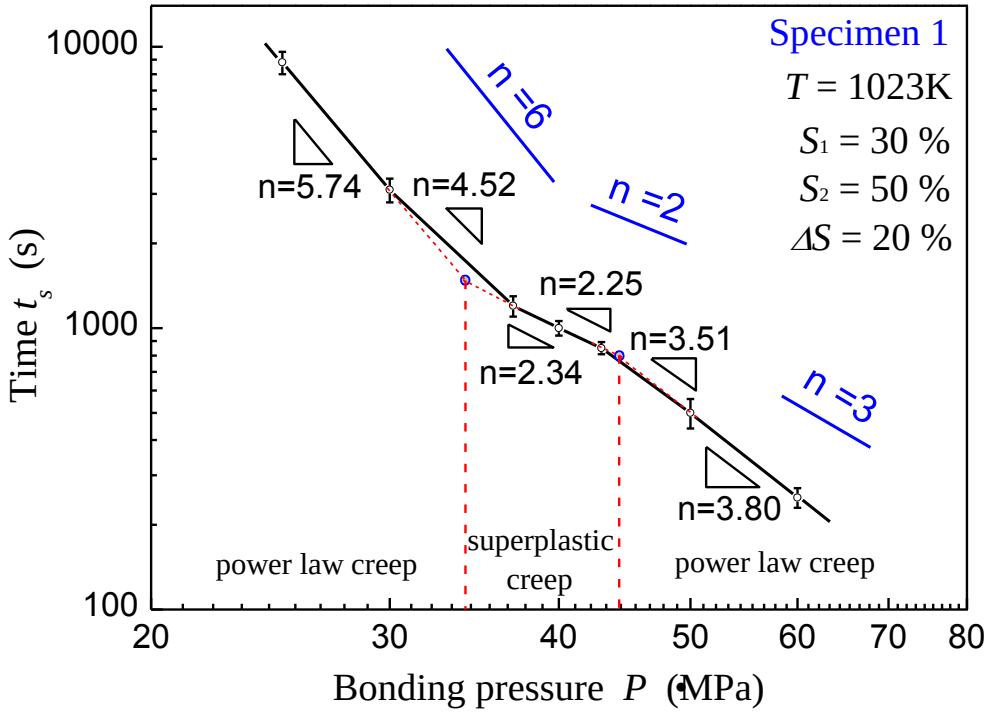

Fig. 4.5 Bonding pressure dependence of t_s (Specimen 1).

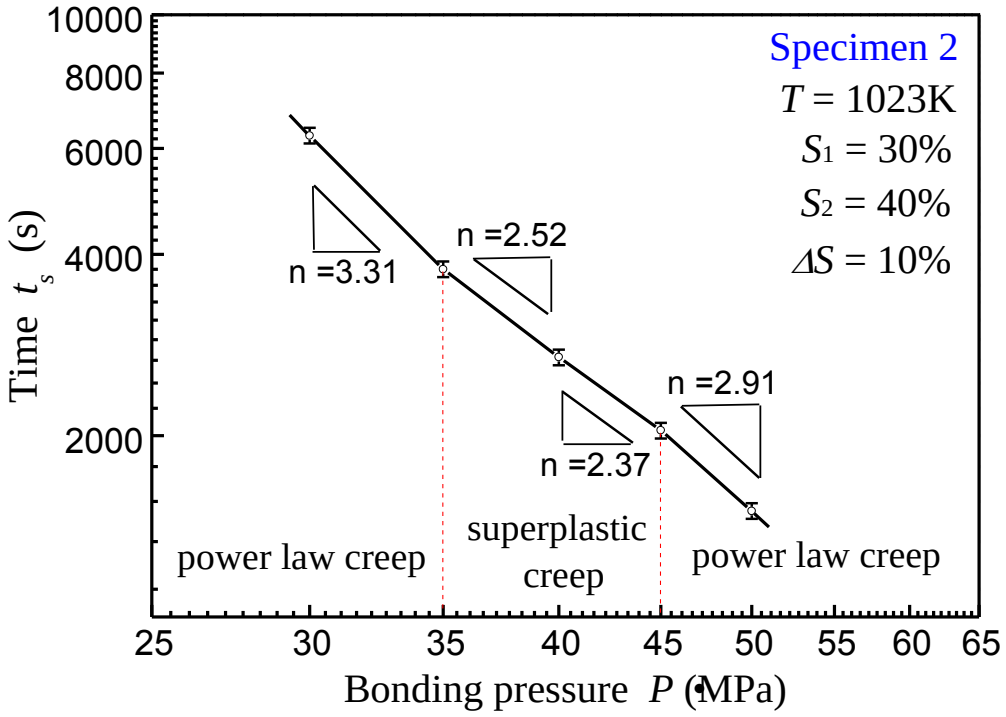

Fig. 4.6 Bonding pressure dependence of t_s (Specimen 2).

This result, P = 35~45MPa, also correlates well to the superplastic flow stress range of SK105 obtained from uniaxial compression tests [6, 7]. It should be noted that the pressure applied to the bonding interface is larger than that of the base metal. However the compression deformation at the bonding interface is more complicated and it is different from uniaxial compression. This agreement of pressure is just for reference. The stress distribution at the bonding interface is needed to be analyze further [3]. Taken together, only when the stress at the bonding interface meets the demand of superplastic flow, the superplastic flow-based deformation occurs at the bonding interface. Superplastic flow can be predominant.

4.2.2 Activation Energy, Q

Fig. 4.7 shows the temperature dependence of T/t_s in Specimen 1. The Q value, measured by the plot log (T/t_s) vs ($1/T$), is about 189 kJmol^{-1} at T = 1003~1023K and 199 kJmol^{-1} at T = 1023~1053K. The Q values are similar in the superplastic range of bonding temperatures (T = 1003~1053K). They are between the activation energy of γ-Fe interfacial self-diffusion (Q_b = 159 kJmol^{-1}) and activation energy of γ-Fe interfacial volume-diffusion (Q_v = 270 kJmol^{-1}) [8]. They are much closer to Q_b. It suggests that the superplastic flow predominantly contributes to the bonding process.

For Specimen 2 (shown in Fig. 4.8), the Q value is about 205 kJmol^{-1} at T = 1023~1053K and 286 kJmol^{-1} at T = 1053~1083K. The Q value increases significantly with the increase in T and that is due to the change in superplasticity at different bonding temperatures. In the case of T = 1023~1053K, which is slightly higher than the critical temperature, this dual-phase fine grained steel shows superplasticity well. The bonding process is controlled by superplastic flow in the superplastic range of temperatures and flow stresses. The Q value during superplastic solid state bonding is much close to Q_b. This is a reliable evidence of the predominance of superplastic deformation, a grain boundary phenomenon, during the interfacial contact process [4, 5]. The most commonly considered mechanisms for superplastic flow involve grain boundary sliding (GBS) and an accommodation process accompanying GBS [9, 10-11]. This fact is well represented by the Q value of both Specimen 1 and Specimen 2.

The grain growth leads to weaker superplasticity at T = 1053~1083K, which is beyond the range of superplastic temperatures. The Q value is closer to the activation energy of γ-Fe volume self-diffusion Q_v. It suggests that the predominant bonding mechanism

turns into power law creep, as explained in next section [4, 5].

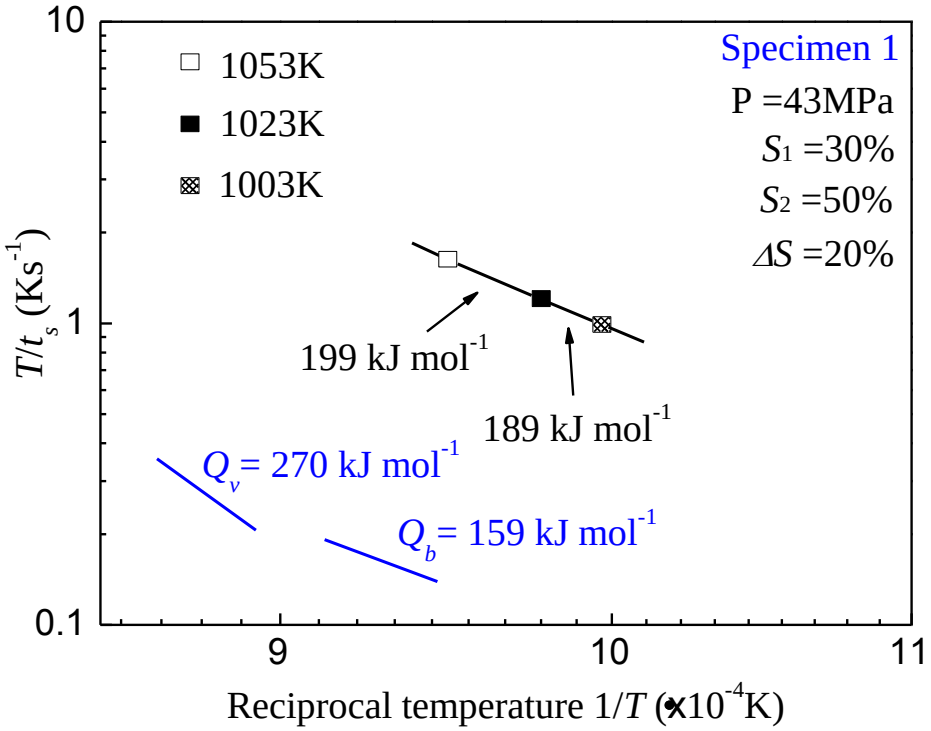

Fig. 4.7 Bonding temperature dependence of T/t_s in Specimen 1.

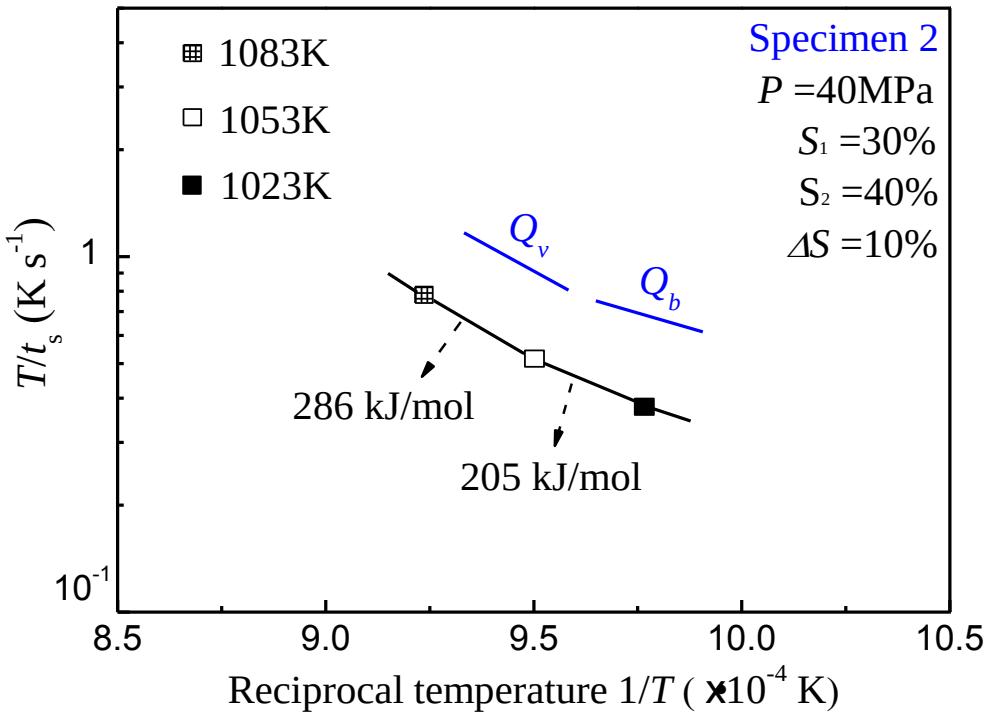

Fig. 4.8 Bonding temperature dependence of T/t_s in Specimen 2.

4.2.3 Microstructure Characteristic

As mentioned in Chapter 1, the microstructure should be steady during the superplastic creep deformation, that is, there is no obvious grain growth and the grain can keep equiaxed after deformation [7, 12]. If superplastic flow is predominant, a typical superplastic microstructure should be maintained. In the present study, after etching by picric acid solution, the interfacial microstructure of superplastic steel after bonding was investigated.

It is difficult to observe the microstructure near the void surface of Specimen 1 clearly due to the small void size and the high carbon content. In the case of Specimen 2, the interfacial microstructure of area A is shown in Fig. 4.9. The austenite grain size keeps constant (less than 10μm) and the grain shape is still equiaxed. This is a typical characteristic of superplastic creep. It can be inferred that the interfacial deformation

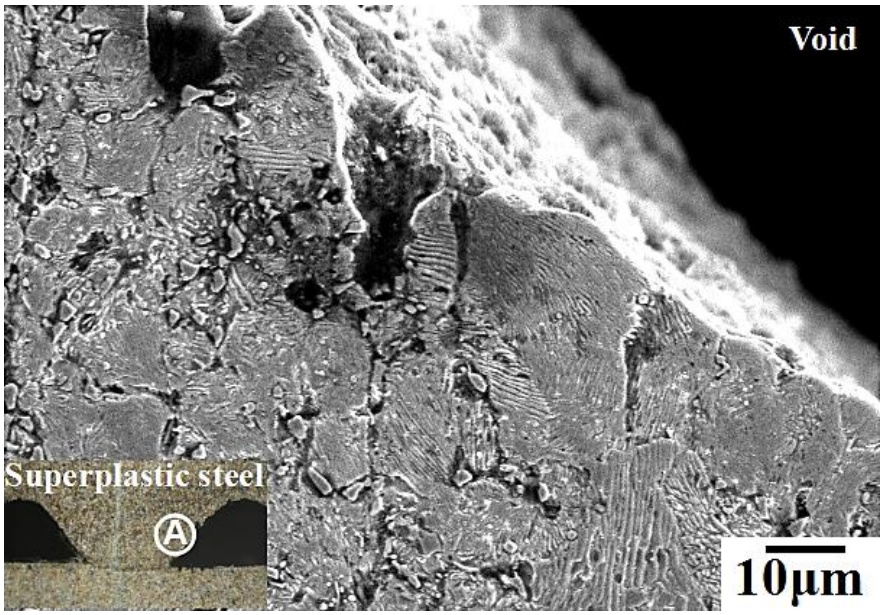

Fig. 4.9 Microstructure of area A in superplastic steel after bonding.

(T = 1023K, P = 40MPa, t = 45min)

contributed to the bonding process is basically superplastic flow. That is, the interfacial contact process is controlled by superplastic flow under the bonding condition ns of superplastic temperatures and pressures.

4.3 Interfacial Contact Process Controlled by Power Law Creep

As described in the previous section, the predominant bonding mechanism can be different because the interfacial stress is always changing during the bonding process. If the interfacial stress is in the range of superplastic flow stress, the superplastic creep can be predominant. Whereas when the interfacial stress is beyond the superplastic flow stress, the bonding process should be controlled by other creep mechanism, that is, power law creep.

4.3.1 Stress Exponent, *n*

As shown in Fig. 4.5, the *n* value of Specimen 1 is large than 4.5 when $P < 37$MPa. It suggests that power law creep is predominant. The *n* value can reach to 5.74 when $P < 30$MPa. This result is also consistent with the value of $n = 6$ provided by Takahashi [2]. The specific value for power law creep is reconfirmed in the present study. The *n* value is lower than 3 when *P* is in the superplastic range of bonding pressure and hence the bonding process is controlled by superplastic flow. Subsequently, as the bonding pressure increases, the *n* value increases further and it is larger than 3.5 when $P > 43$MPa. The creep mechanism becomes increasingly influential and the effect of

superplastic flow is weakened significantly. The predominant mechanism thus in effect comes back to exhibit power law creep [4, 5].

For Specimen 2, as shown in Fig. 4.6, the n value is about 3.31 when P < 37MPa. In the case of such bonding pressures, the interfacial deformation should be made up of common creep (power law creep) and superplastic creep. Superplastic flow is not yet predominant, though it occurs at the bonding interface more or less. The power law creep-based deformation predominantly contribute to the bonding process. The n value decreases gradually as the pressure increases, as a result of a change in the predominant bonding mechanism. The n value is about 2.5 (m = 0.4) for the bonding pressure P = 35~45MPa.

The interfacial contact process is assuredly controlled by superplastic flow. The n value increases gradually as P increases further and it is close to 3 when P > 45MPa, the effect of superplastic flow on interfacial contact process decreases and the power law creep mechanism becomes increasingly influential.

4.3.2 Active Energy, Q

As shown in Fig. 4.8, in the case of Specimen 2, the values of Q are very different at different ranges of bonding temperature. It is due to the change in predominant bonding mechanism.

When T = 1023~1053K, which is in the range of superplastic-causing temperatures, the superplastic flow-based deformation occur under appropriate bonding pressures. The Q value during superplastic solid state bonding is much close to Q_b. as the same as Specimen 1. With increasing T, more carbides are dissolved, and hence the limiting

effect of second phases (fine carbide) on grain growth is weakened. The stability of grain size concomitantly reduces. In the case of T = 1053~1083K, the superplastic steel cannot show superplastic behavior at such high temperatures. The interfacial deformation is mainly common creep. The Q value is basically equal to the activation energy of γ-Fe volume self-diffusion, Q_v. It suggests that the interfacial contact process is controlled by power law creep [3-5].

It can be also inferred that if T is relatively lower than the superplastic temperature, for instance, T < 1003K, the superplastic flow should be restrained. The predominant bonding mechanism must be power law creep under the same condition of bonding pressure.

4.3.3 Microstructure Characteristic

Chapter 2 presents several mechanisms for high temperature deformation. For the solid state bonding of high carbon steel, if the interfacial deformation is climb-controlled creep, the grain can be elongated in the direction of plastic flow and the grain growth can be also observed [13]. This is a typical microstructure of common creep deformation.

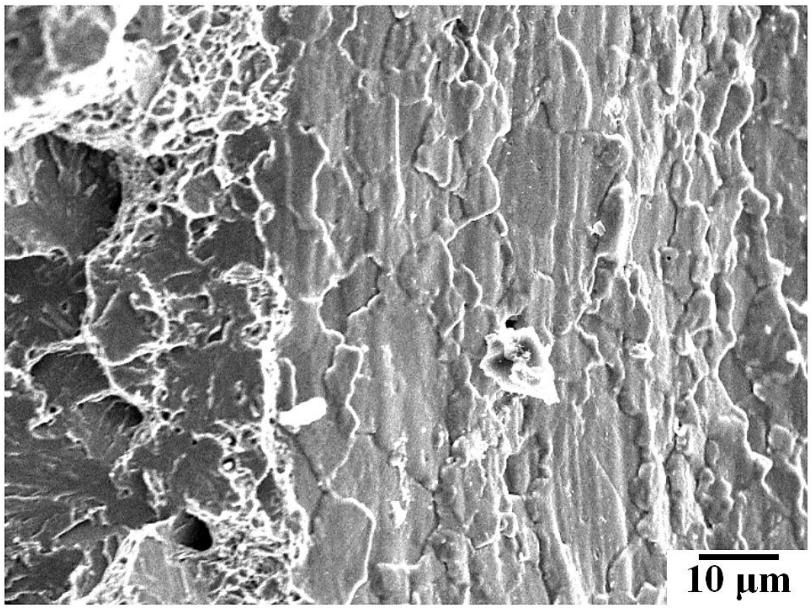

Fig. 4.10 Void surface of Specimen 2 after bonding.

(T = 1023K, P = 45MPa, t = 50min)

In the same way, the interfacial microstructure (void surface) of Specimen 2 after bonding is shown in Fig. 4.10. Obviously, the microstructure after bonding changes. The microstructure characteristics of climb-controlled creep including slight grain growth, and grain deformation are obtained. It suggests that the bonding process is controlled by power law creep.

4.4 Effect of Geometrical Factors of Surface Asperity

If the visco-plastic deformation mechanisms, such as power law creep or superplastic flow, are predominant, the actual bonding process can be affected by the geometrical factor: initial void shape with the surface asperity angle α_{00} (as shown in Fig. 2.4 (a) before bonding).

The initial void shape is changed by the angle α_{00} and the interfacial contact mode can

also be changed by the initial void shape. That is, surface folding (mode I) is dominant in the region of α_{00} < 30 deg; interfacial expansion (mode II) is dominant in the region of α_{00} > 45 deg; both of surface folding and interfacial expansion (mode transition I-II) work, for α_{00} = 30~45 deg [14, 15].

The interfacial contact modes controlled by power law creep have been confirmed experimentally [15]. However, there has been an unclear point for the solid state bonding of superplastic materials. It is necessary to confirm the effect of geometrical factors on the contacting modes due to the superplastic flow. A better understanding of bonding process can be obtained.

It was difficult to make the void more sharp (α_{00} > 50 deg) due to the hardness of high carbon steel SK105. Specimen 1 (α_{00} = 30 deg) and Specimen 2 (α_{00} = 45 deg) are therefore adopted to do a comparison, thus analyzing the influence of initial void shape on the interfacial contact process during superplastic solid state bonding.

In consideration of the slight inward shrinkage of original steel by instantaneous plastic deformation, the actual surface asperity angle α_0 should be slightly less than the angle α_{00} of initial void shape. In such experimental condition, the angle α_0 is supposed to be constant in a relatively narrow range of bonding ratio increment. In case of Specimen 2, the void shrinkage ΔV is exactly measured by the void area, while the bonding ratio S is measured by the fracture surfaces. The ΔV dependence of the bonding ratio S is shown in Fig. 4.11.

As seen in this figure, the 13.3% initial binding ratio is obtained by instantaneous plastic deformation at +0s. The void shrinkage ΔV increases with the bonding ratio S during

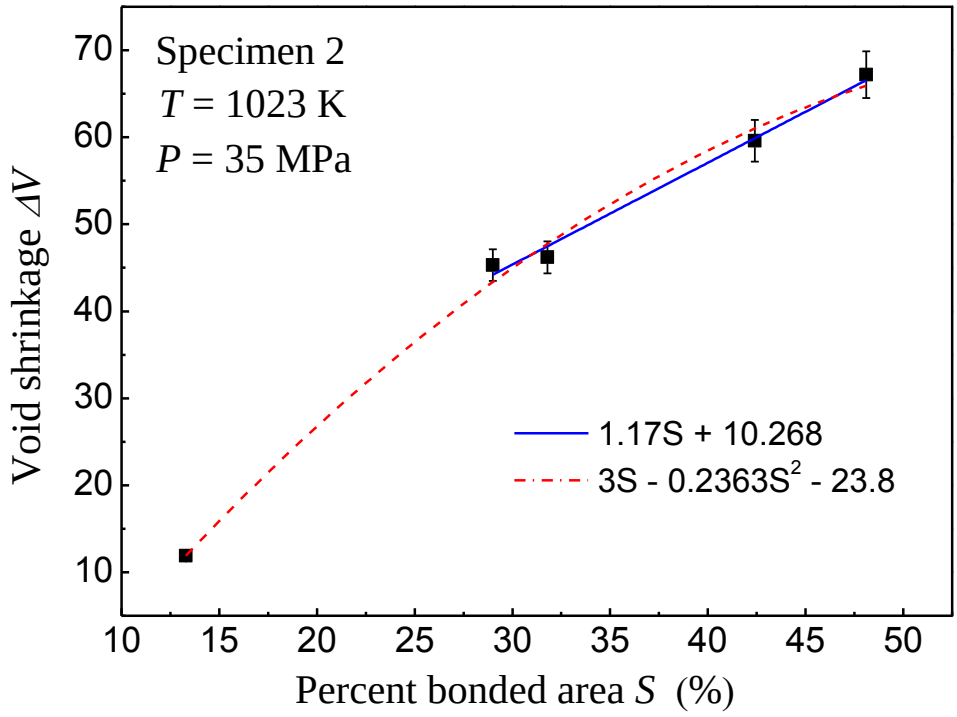

Fig. 4.11 Void shrinkage dependence of the bonding ratio *S*

the whole bonding process (*S* < 50%). The analysis result shows that the growth of ΔV is as quadratic function curve (red dotted line). While in a relatively narrow range of bonded area, *S* = 32~48% shown in this figure, the linear relationship between *S* and ΔV (blue solid line) is presented. It suggests that the ΔV is roughly proportional to bonding ratio *S* due to the single predominant bonding mechanism, superplastic flow. In other word, the angle α_0 keeps constant during the bonding process from Stage 1 to Stage 2. The prerequisite of the identification model shown in Section 2.3 is confirmed [4].

The contact processes of both Specimen 1 and Specimen 2 are shown in Fig. 4.12 and Fig. 4.13 respectively. The deformation for void shrinkage mainly occurs on the side of superplastic steel and the void shape keeps approximately constant during the bonding processes.

Fig. 4.12 illustrates the void shrinkage process with small surface asperity angle α_{00} = 20 deg of Specimen 1. Relatively large instantaneous plastic deformation occurs in the area of primary contact due to the high pressure. The void tip surface formed by original steel slightly shrinks inward and hence the actual surface asperity angle α_0 is slightly less than the angle α_{00} of initial void shape. This type of narrow void can be described as Lens-type (α_0 = 10~15 deg). The bonding ratio S_1 = 30% is obtained when the bonding time t = 800s and S_2 = 50% is obtained while t = 1800s. The bonding increases rapidly as the bonding time increases in Lens-type process. The bonding rate dS/dt of Specimen 1 can be roughly equal to $2\times10^{-4}s^{-1}$ when S = 30~50% [3, 4].

The interfacial contact process of Specimen 2 is shown in Fig. 4.13. The area A near the void surface of superplastic steel is adopted to investigate the typical microstructure

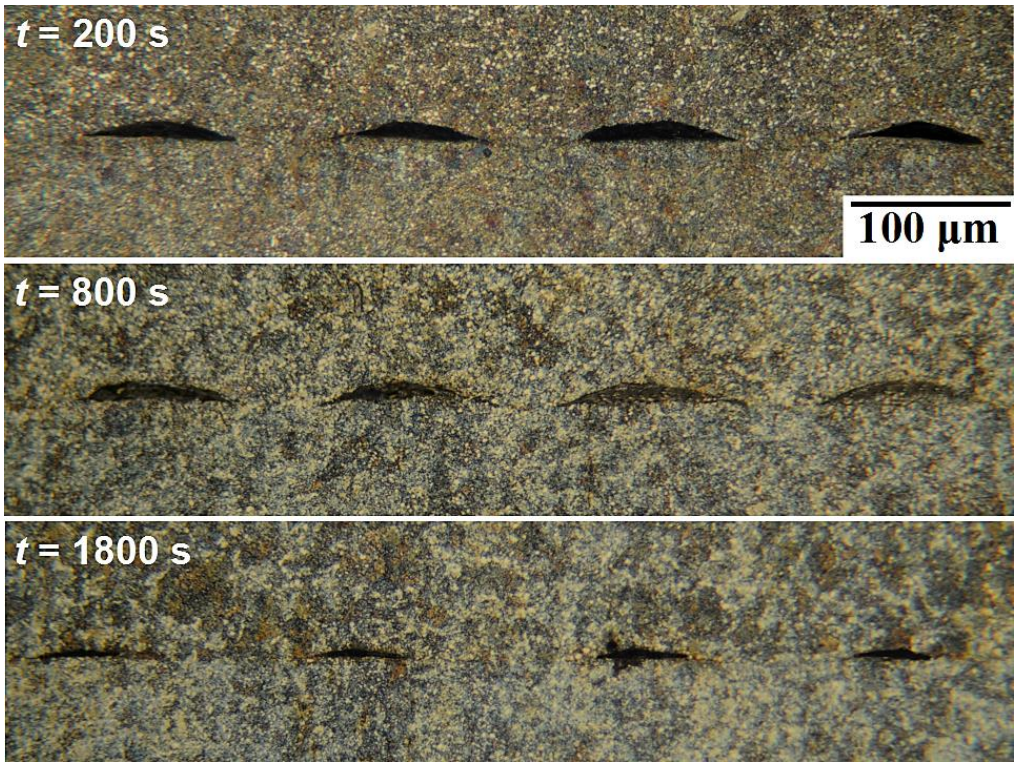

Fig. 4.12 Lens-type contact process of Specimen 1 (1023K, 40MPa).

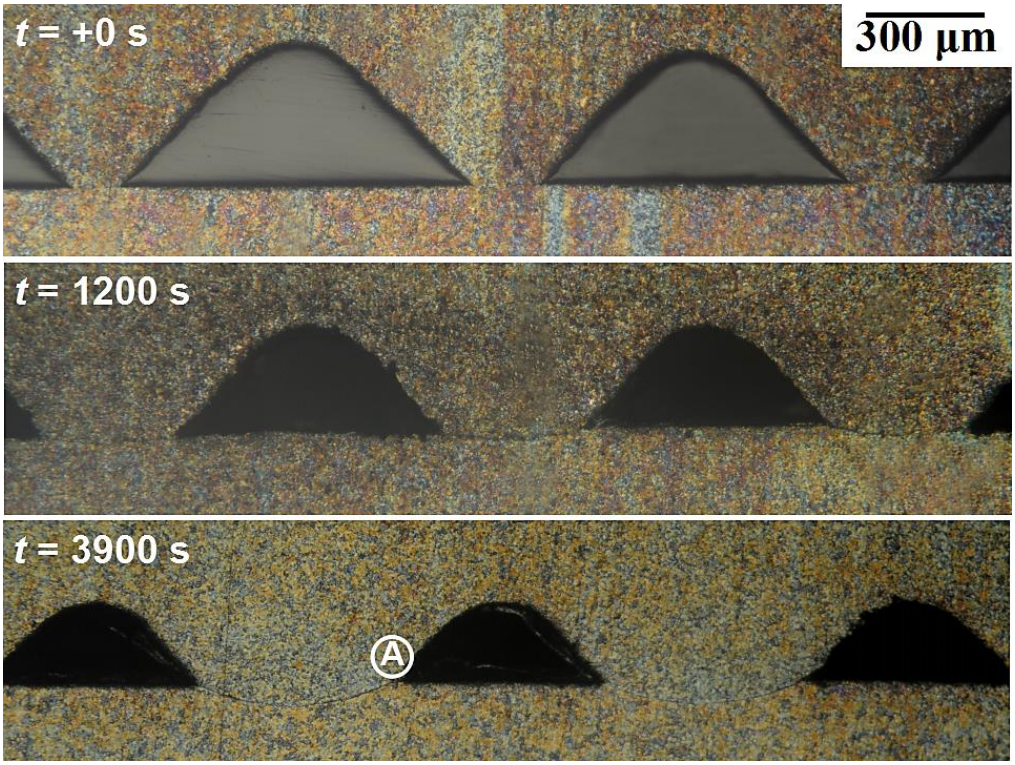

Fig. 4.13 Massif-type contact process of Specimen 2 (1023K, 40MPa).

characteristic of superplastic behavior (as shown in the inset of Fig. 4.9). For the convenience of measuring S and ΔV, the larger L_{00} and α_{00} are adopted in Specimen 2. Like the Lens-type process, the asperity angle of void shape during the bonding process is slightly less than the in initial value α_{00}. This type of sharp void can be described as Massif-type (α_0 = 40~45 deg). The void shrinkage is uniform as the bonding time increases. The bonding ratio S_1 = 30% is obtained when the bonding time t = 1200s and approximately 40% bonding ratio is finally obtained while t = 3900s. The average bonding rate of Specimen 2 is about $3.7\times10^{-5}s^{-1}$ when S = 30~40% [4, 5].

By comparing these two types of interfacial contact processes, there is a significant difference of bonding rate and it is due to the effect of void shape with the surface asperity angle α_0. The bonding rate of Lens-type is 5 times larger than that of Massif-type. This is the effect of geometrical factor on the bonding process.

According to the finite element model proposed by Takahashi [15], there are two modes of visco-plastic interfacial contact process. One of them is the void surface folding which becomes dominant for fine surface asperity (α_0 < 30 deg). The other is the interfacial expansion of the bond interface which becomes dominant for sharp surface asperity (α_0 > 45 deg).

The experimental results show that high bonding rate is achieved in the Lens-type contact process due to the surface folding (mode I) for α_0 = 15~20 deg. In the mode of surface folding, the faying surface overlaps readily and the bonding ratio increases rapidly with the bonding time. However, the contacting mode turns into interfacial expansion (mode II) with the α_0 increases. In the mode transition I-II (α_0 = 30~45 deg), the bonding process is affected by both of surface folding and interfacial expansion while the bonding rate is inhibited at the middle stage of bonding (S = 35~70%) [4, 15]. For the Massif-type contact process, α_0 is relatively large. Although the void top folding occurs, the bonding rate is inhibited due to the low void tip folding (shown in Fig. 2.4(a)). Therefore, low bonding rate is obtained due to the constraint by mode transition I-II for α_0 = 40~45 deg. This result agrees well with the numerical simulation [15].

These two contacting modes produce the effect of the initial void shape on the interfacial contact process and change the bonding rate distinctly. Assuming more sharp initial void shape with larger surface asperity angle (α_0 > 60 deg) is adopted, it can be inferred that the bonding process is controlled by interfacial expansion completely and the bonding rate is similar as that of mode I, although contacting modes are different [14, 15].

It is important to note that, the change in bonding mechanisms keep constant even the bonding surfaces are different. In other words, the geometrical factor of surface

roughness (void shape) don't change the predominant bonding mechanisms and it can only influence the bonding process.

4.5 Conclusions

The solid state bonding of superplastic steel and original steel with different initial void shapes was investigated under different bonding conditions. The bonding process was analyzed by characteristic value of *n*, and *Q*. Two predominant bonding mechanisms for solid state bonding were discussed on the basis of the identification model. The discussion is summarized as follows.

1) The predominant bonding mechanisms can be identified by measuring the stress exponent, *n* value and activation energy, *Q* value.
2) Superplastic flow played a dominant role during the interfacial contact process from a bonding ratio of 30% to 50%, under the conditions of bonding temperature T = 1023~1053K and bonding pressure P = 35~45MPa. The superplastic solid state bonding is just produced in the middle bonding stage under the conditions of T = 1023~1053K and P = 35~45MPa.
3) Superplastic deformation cannot be always predominant even though it occurs during the solid state bonding of superplastic steel. If the bonding temperatures and the interfacial flow stresses are out of the appropriate range for superplastic flow. The bonding process should be controlled by power law creep.
4) The bonding process is similarly affected by the geometrical factor: initial void

shape with the asperity angle α_0. Surface folding is dominant during the Lens-type contact process of α_0 = 10~15 deg which shows a high bonding rate. On the other hand, the Massif -type contact process of α_0 = 40~45 deg is controlled by both surface folding and interfacial expansion modes. Meanwhile, a low bonding rate is achieved due to the constraint of contact process. The different contacting modes produce the effect of the void shape as a geometrical factor on the interfacial contact process and change the bonding rate.

5) The geometrical factor of surface roughness (void shape) can just influence the bonding process and it is independent to the bonding mechanism. In other words, even if the surface roughness changes, the identification of the predominant bonding mechanism is established.

References

[1] Y. Takahashi: Ceramic Trans., 2003, Vol. 138, pp. 29-47.

[2] Y. Takahashi, K. Inoue and K. Nishigushi: Acta Metall., 1993, Vol. 41, pp. 3077-3084.

[3] Z.H. Heng, M. Maeda and Y. Takahashi: IOP Conf. Series: Mater. Sci. Eng., Doc.No. 61(2014)012003.

[4] Z.H. Heng, T. Matsushima, Y. Nashiki, M. Maeda and Y. Takahashi: Journal of Smart Processing., 2015, Vol. 4, pp. 102-108.

[5] Z.H. Heng, T. Matsushima, Y. Nashiki, M. Maeda, K.K. Zhang and Y. Takahashi: Quarterly Journal of the Japan Welding Society., 2015, Vol. 33(2), pp. 67-70.

[6] Y.L. Yang, K.K. Zhang, C.S. Wang, N. Zhao and X.M. Xu: J. Iron. Steel. Res., 2004, Vol. 16(6), pp. 65-68. (in Chinese)

[7] K.K. Zhang: Study on Technology of Isothermal Superplastic Solid State Welding., 2002, pp. 29-33. (in Chinese)

[8] James DW and Leak GM: Phil. Mag., 1965, Vol. 12, pp. 491.

[9] Y. Maehara, TG. Langdon: Mater.Sci.Eng., 1990, Vol. 128, pp. 1.

[10] TG. Langdon: Phil.Mag., 1970, Vol. 78, pp. 689.

[11] RC. Gifkins: Metall Trans., 1976, Vol. 7, pp. 1225.

[12] Nieh TG: Superplasticity in Metals and Ceramics., 1997, Cambridge University Press, New York.

[13] F. Garofalo: Fundamentals of Creep and Creep-Rupture in Metals., 1966, Macmillan, New York.

[14] Y. Takahashi and M.Tanimoto: Trans. ASME J. Eng. Mater. Technol., 1995, Vol. 117, pp. 336-340.

[15] Y. Takahashi and M.Tanimoto: Trans. ASME J. Eng. Mater. Technol., 1995, Vol. 117, pp. 330-335.

Chapter 5: Bonding Process Controlled by Diffusional Mechanism

In previous chapter, the interfacial contact process controlled by high temperature deformation in the middle bonding stage has been discussed. As bonding process continues, the interfacial stress decreases with the increase in bonding ratio. The diffusional mechanism such as interface self-diffusion and volume self-diffusion becomes dominant in the final bonding stage rather than the deformation mechanisms [1]. In this chapter, the solid state bonding of superplastic steel (Specimen 3) with fine bonding surfaces and original steel is investigated. The bonding process controlled by Newtonian deformation due to vacancy diffusion flow can be identified by the characteristic values of n, and Q.

5.1 Bonding Results

Newtonian deformation dominates the bonding process under the conditions of relatively low bonding pressures and fine bonding surfaces [1, 2]. Therefore, Specimen 3 is adopted to bond with original steel and the bonding results are shown as follows. Fig. 5.1 shows the bonding surfaces of superplastic steel at different bonding stages. As shown in Fig. 5.1(a), the ridges on the bonding surface made by abrasive (emery) paper are not uniform. The void distance can be estimated by the linear intercept method, that is, the void points in unit distance (red points shown in this figure) are calculated and

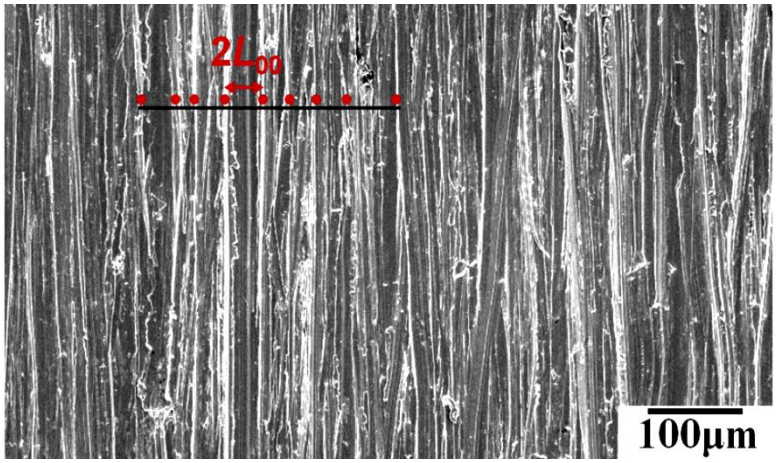

(a) Initial surface before bonding

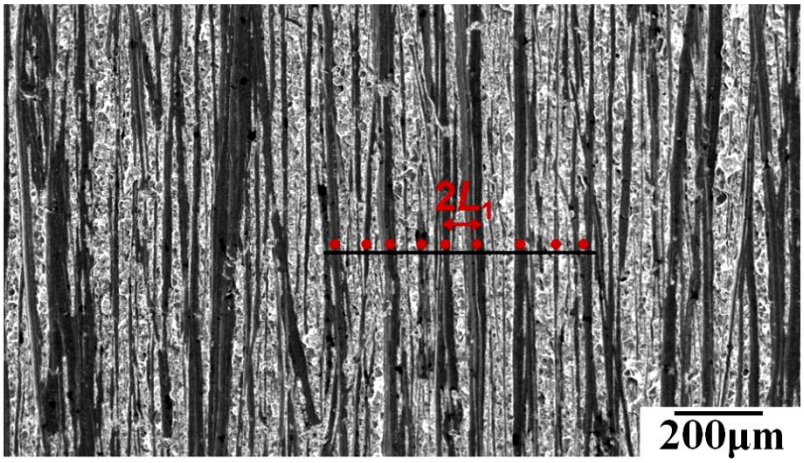

(b) Fractured surface at Stage 1

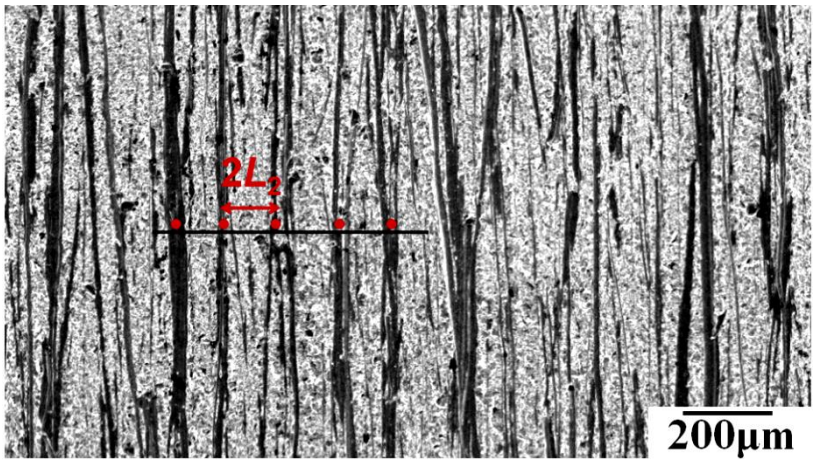

(c) Fractured surface at Stage 2

Fig. 5.1 SEM observation of bonding surfaces (Specimen 3).

the average value range ($2L_{00}$ = 15~30 μm) can be obtained. The half void distance L can also change during the bonding process due to the uniform distribution of ridges. From the Fig. 5.1(b) and (c), the bonded area can be distinguished by the bright zone and the void surface is marked by the dark zone. The bonding ratio can be estimated by the percentage of bright area.

When the bonding pressure is 40MPa and the bonding time t_1 is 30mins, the bonding ratio S_1 = 65% is obtained by the creep deformation and it is set as Stage 1. The half void distance is marked as L_1. And then, the bonding process continues under relatively low pressures. The diffusional mechanisms can therefore be predominant. When the bonding ratio increment ΔS = 7%, S_2 = 72% is set as Stage 2 and the half void distance

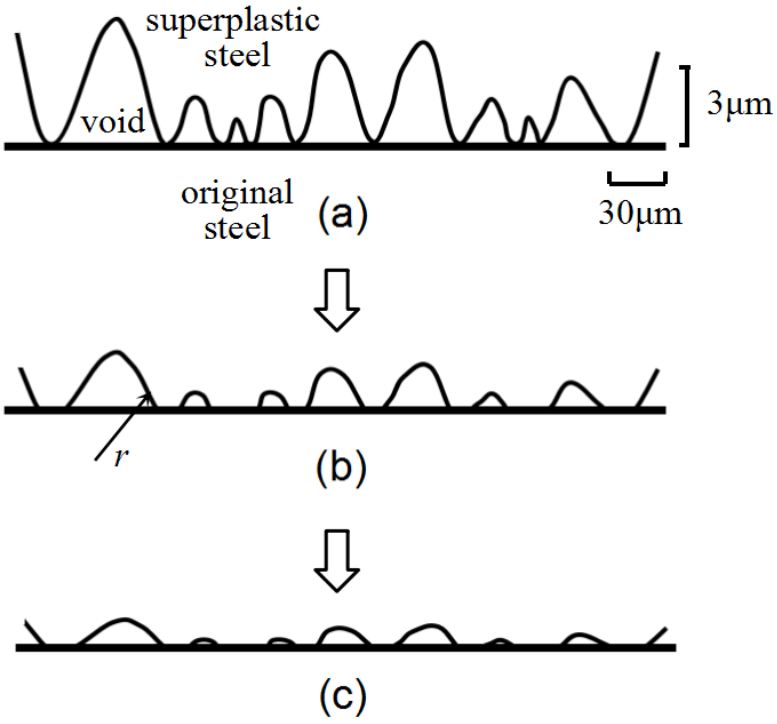

Fig.5.2 Schematic illustration of bonding process.

(a) Initial stage, (b) Stage 1, and (c) Stage 2.

Table 5.1 Bonding surfaces at different bonding stages.

Stage	Bonding time	Bonding ratio	Half void distance	Estimated value of L
Initial	0	0	L_{00}	8~15 μm
1	t_1	S_1 = 65%	L_1	10~20μm
2	t_2	S_2 = 72%	L_2	30~60μm

increases to L_2 as shown in Fig. 5.1(c). The bonding process is schematically illustrated in Fig. 5.2 and the geometrical factor of half void distances at different bonding stages are shown in Table 5.1.

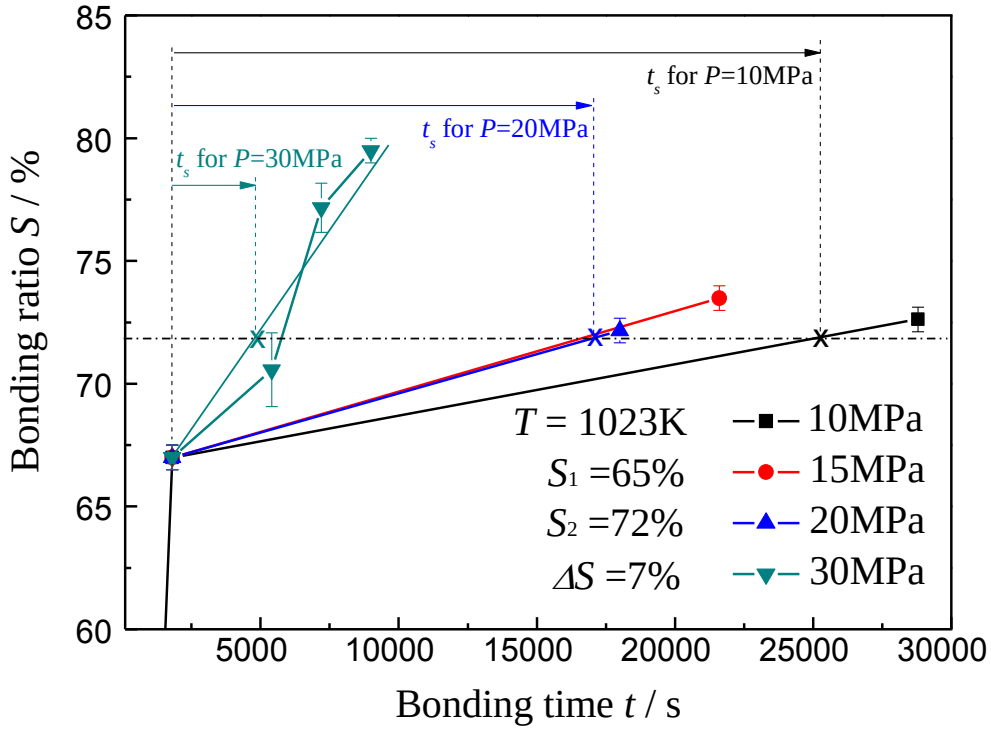

Fig. 5.3 Bonding time dependence of bonding ratio.

Fig. 5.3 shows the bonding results at 1023K under different bonding pressures. Relatively long bonding time t is required to obtain a certain bonding ratio increment under low pressure. The linear relationship between bonding ratio S and bonding time t is also obtained. The interpolation method explained in Section 3.3 can be possible. That is, the dot-dashed line for S = 72% shown in this figure can be inserted to estimate the bonding time t_2 for stage 2. The time t_s, which is from Stage 1 to Stage 2, can be calculated for investigating the predominant bonding mechanism.

5.2 Interfacial Contact Process Controlled by Diffusional Mechanism

The characteristic values of n and Q during the bonding process can be calculated by the time t_s as Specimen 1 and Specimen 2.

5.2.1 Stress Exponent, n

Fig. 5.3 shows the bonding pressure dependence of t_s under the conditions of T = 1023K and relatively low bonding pressures. As shown in this figure, the value of n changes with the bonding pressure. When the bonding pressure P = 10~20MPa, the n value is about 0.6 and it is less than unity. It suggests that the bonding process is controlled by diffusional mechanism (Newtonian deformation) and there is no creep deformation for the interfacial contact process. With the bonding pressure increases, the dislocation creep deformation becomes more important to the bonding process. The value of n can research to 1.6 for P = 20~30MPa and it suggests that a combined effect of two or more fundamental mechanisms act on the void shrinkage process.

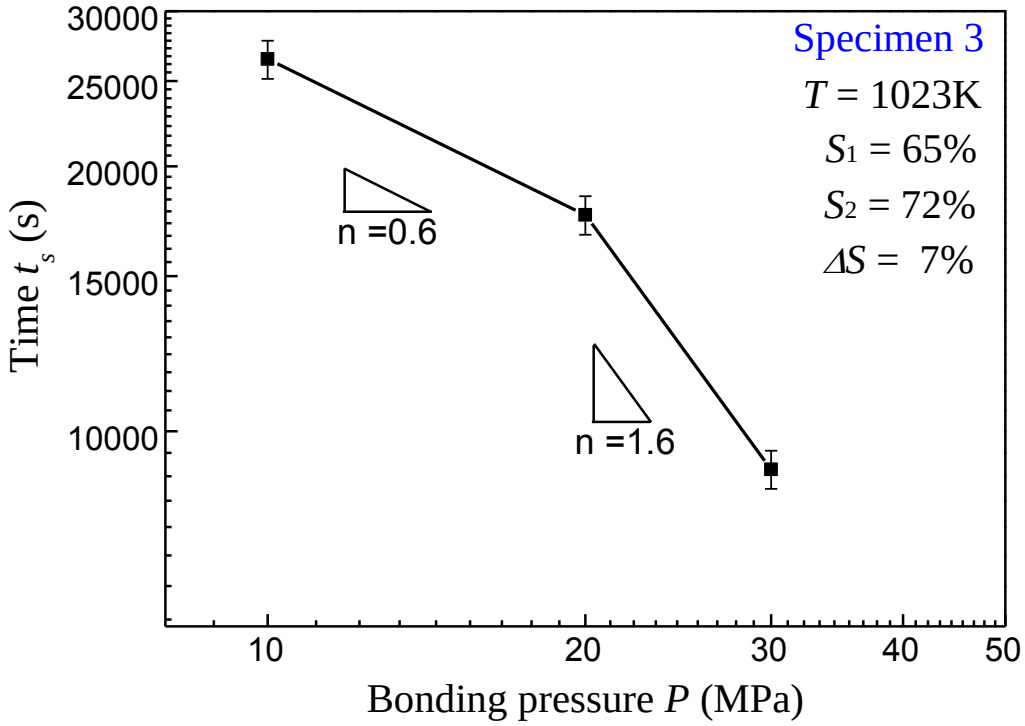

Fig. 5.4 Bonding pressure dependence of t_s (Specimen 3).

In the case of P = 10~20MPa, the interfacial stress is low enough for the dislocation creep to be ignored in the final bonding stage. So that the dislocation creep cannot occur in the final bonding stage (S > 65%). In other words, the diffusional mechanism can be predominant. The void shrinkage rate $(\mathrm{d}V/\mathrm{d}t)_{\mathrm{diff}}$ due to the diffusional mechanisms (interface self-diffusion and volume self-diffusion) is expressed [2, 3] by

$$\left(\frac{\mathrm{d}V}{\mathrm{d}t}\right)_{diff} = \frac{6\Omega}{kTSX}\left(\frac{\sigma}{S} - \frac{\gamma_s}{r}\right)\left(\delta_b D_b + \frac{2L}{\pi} D_v\right) \qquad (5\text{-}1)$$

where Ω is the atom volume, k is Boltzman's constant, σ is the interfacial stress the sign of which is minus (P = - σ), γ_s is the surface tension, r is the curvature radius of void tip as shown in Fig. 5.2, δ_b is the thickness of interface diffusion layer, D_b is the interface (grain boundary) self-diffusion coefficient, and D_v is volume self-diffusion

coefficient. The initial bonding surface of Specimen 3 is so fine that r is large enough. If the term (γ_s/r) is much less than (σ/S), the t_s is proportional to $1/P$ and $n = 1$ can be obtained. As the bonding process continues, the void shape changes to be compressed and r decreases. When the term (γ_s/r) is not negligible, the n value less than unity can be obtained [2].

In the case of P = 20~30MPa, the value of n is larger than unity. It suggests the interfacial contact is contributed not only by Newtonian deformation but also by dislocation creep deformation. That is, power law creep deformation is expected to occur more or less at the bonding interface. As the bonding pressure increases further, the effect of dislocation creep deformation can be more important and the predominant bonding mechanism can change to power law creep.

5.2.2 Activation Energy, Q

The activation energy Q during the bonding process can be calculated by the time t_s at different bonding temperatures from equation (2-5).

Fig. 5.5 shows the bonding temperature dependence of T/t_s in Specimen 3 under P = 20MPa. The Q value, measured by the plot log (T/t_s) vs ($1/T$), is about 311 kJmol^{-1} at T = 1023~1053K while it is about 263 kJmol^{-1} at T = 1053~1083K. The activation energy of Q = 288 kJmol^{-1} can be obtained in the whole range of bonding temperatures. The value of Q is close to or larger than Q_v during the bonding process [4]. It suggests that the volume self-diffusion predominantly contributes to the void shrinkage process.

It is well known that the diffusion in superplastic materials with fine grain size is

interface (grain boundary) self-diffusion based [5, 6]. However, the experimental results show that the volume self-diffusion dominates the bonding process. It is due to the change in void distance. As mentioned in previous section, the void distance of 2*L* increases obviously because the void ridges at bonding surface are not uniform.

From the equation (5-1), the term ($2LD_v/\pi$) can increase with the increase in *L* and the volume self-diffusion becomes more important. The void shrinkage should hence be controlled by volume self-diffusion.

Furthermore, the bonding process is also influenced by the bonding materials. In such bonding condition, the original steel with coarse microstructure is adopted to bond with the superplastic steel. Fig. 5.6 shows the diffusion occur at the bonding interface between the superplastic steel and original steel. The bonded area with high vacancy

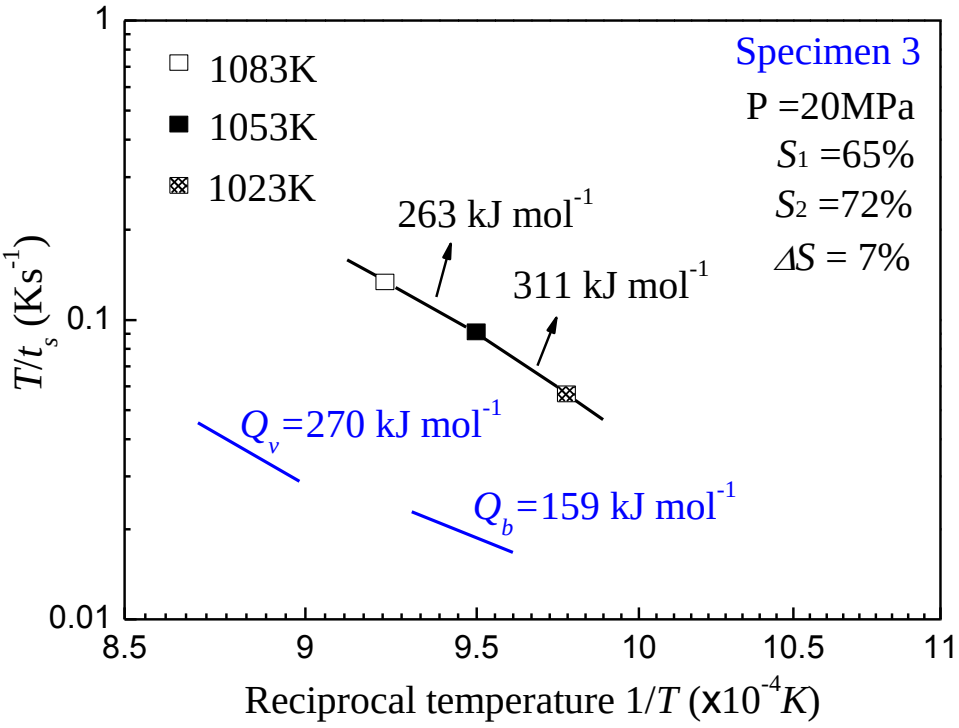

Fig. 5.5 Bonding temperature dependence of T/t_s in Specimen 3.

density is marked by the red line. The atoms diffuse to the void surface. In the fine grained superplastic steel, the abundant grain boundaries offer the diffusion path for void shrinkage. Therefore, the diffusion in superplastic steel is mainly interface self-diffusion [5, 7]. On the other side, the grain size of original steel is larger than the void size, the diffusion in original steel should be volume self-diffusion based. Assuming the effect of diffusion in both sides are equivalent, the volume self-diffusion can be dominant and the experimental result of Q value, which is close to Q_v, is credible.

In the case of solid state bonding between superplastic steel and superplastic steel, the diffusion process contributed to the void shrinkage should be controlled by the interface self-diffusion and the activation energy Q during the bonding process is close to Q_b can be predicted.

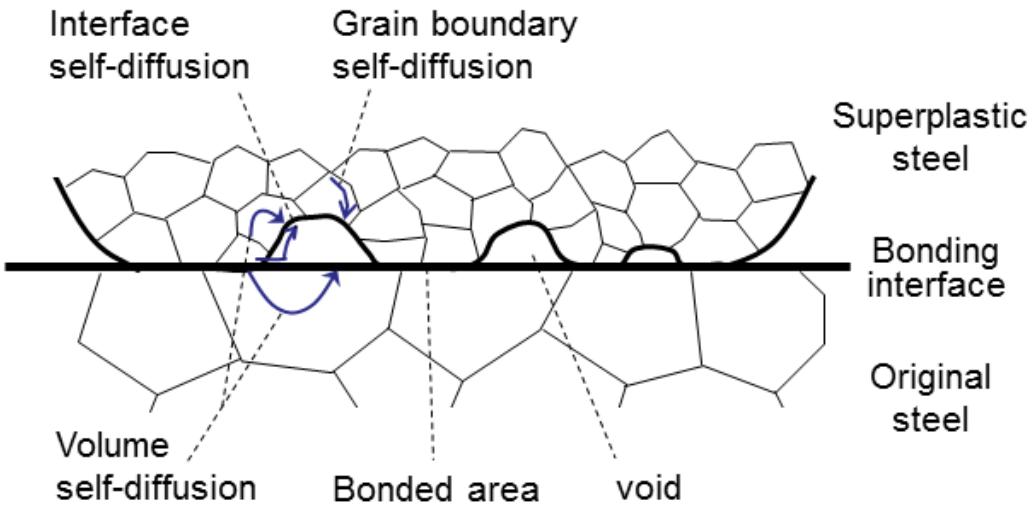

Fig. 5.6 Schematic illustration of diffusion for void shrinkage.

5.3 Conclusions

The solid state bonding of superplastic steel and original steed in the finial bonding stage was investigated. The bonding process controlled by diffusional mechanisms was identified by the characteristic values of n and Q. Two fundamental diffusional mechanisms for solid state bonding were also discussed. The summary of discussion is as follows.

1) The predominant bonding mechanism can be identified by the characteristic value of n, and Q during the bonding process.
2) Diffusional creep predominantly contributes to the interfacial contact process from a bonding ratio of 65% to 72%, under the conditions of relatively low bonding pressure P = 10~20 MPa and bonding temperature T = 1023~1083K.
3) If the diffusional mechanism is predominant, the value of n is equal to unity and it can be less than unity due to the flattening of void shape.
4) The diffusion type can be also distinguished by the active energy Q value. In other words, the value of Q is much close to Q_b when the grain boundary self-diffusion dominates. While the value of Q is much close to Q_v in the case of volume self-diffusion based Newtonian deformation is predominant.
5) For the solid state bonding between superplastic steel and original high carbon steel, the bonding mechanism under low bonding pressures can be controlled by diffusional creep and influenced by grain size of the original steel. The predominant bonding mechanism depends on the combined effect of both bonding materials.
6) Even though the bonding materials can show superplasticity behavior and the

superplastic flow can occur during the bonding process, the diffusional bonding mechanisms are predominate in the final bonding stage for a sound bond.

References

[1] Y. Takahashi: Ceramic Trans., 2003, Vol. 138, pp. 29-47.

[2] Y. Takahashi, K. Inoue and K. Nishigushi: Acta Metall., 1993, Vol. 41, pp. 3077-3084.

[3] Y. Takahashi and K. Inoue: Journal of High Temperature Society., 1997, Vol. 23, pp.179-189.

[4] James DW and Leak GM: Phil. Mag., 1965, Vol. 12, pp.491.

[5] Nieh TG: Superplasticity in Metals and Ceramics., 1997, Cambridge University Press, New York.

[6] Z.H. Heng, M. Maeda and Y. Takahashi: IOP Conf. Series: Mater. Sci. Eng., Doc.No. 61(2014)012003.

[7] RC. Gifkins: Metall Trans., 1976, Vol. 7, pp. 1225.

Chapter 6: Conclusions

The present research focused on the superplastic deformation in the solid state bonding and its effect on the interfacial contact process. The solid state bonding of fine grained high carbon steel SK105 with different surface roughness was investigated using the existing identification model. The predominant bonding mechanisms in different bonding stages were identified by the characteristic values of n and Q. The influence of geometrical factors of surface asperity and microstructure on the bonding process were also discussed.

In Chapter 1, the superplasticity behavior of Fine-structure materials and its evaluation indexes were explained at first to show the advantages of superplastic materials for the solid state bonding. In the next step, the solid state bonding and its modeling were overviewed extensively and the current researches on solid state bonding of superplastic materials were introduced. The identification of predominant bonding mechanism and the description of the effect of superplastic flow were extracted as the objective. A better understanding of solid state bonding with superplasticity can be described and the bonding process can be predict and optimized.

In Chapter 2, the basic theories of high temperature deformation and the bonding mechanisms were described. The identification model of predominant bonding mechanism was also explained in detail.

In Chapter 3, the experimental procedure employed in the present study was described. The selection of high carbon steel and its preparation for superplasticity were exhibited at first. The requirements for superplastic flow were investigated to determine the

bonding conditions. The bonding specimens with different bonding surfaces were prepared for the solid state bonding. The measurement method for the characteristic value of *n*, and *Q* and the characteristic microstructure after bonding were also described.

In Chapter 4, the solid state bonding of superplastic steel and original steel with different initial void shapes was investigated under different bonding conditions. The bonding process was analyzed by characteristic value of *n*, and *Q*. Two predominant bonding mechanisms for solid state bonding in the middle bonding stage were discussed. The following points were clarified.

1) The predominant bonding mechanisms can be identified by measuring the stress exponent, *n* value and activation energy, *Q* value. Superplastic flow played a dominant role during the interfacial contact process from a bonding ratio of 30% to 50%, under the conditions of bonding temperature T = 1023~1053K and bonding pressure P = 35~45MPa. The superplastic solid state bonding is just produced in the middle bonding stage under the conditions of T = 1023~1053K and P = 35~45MPa.
2) Superplastic deformation cannot be always predominant even though it occurs during the solid state bonding of superplastic steel. If the bonding temperatures and the interfacial flow stresses are out of the appropriate range for superplastic flow. The bonding process should be controlled by power law creep.
3) The bonding process is similarly affected by the geometrical factor: initial void shape with the asperity angle α_0. Surface folding is dominant during the Lens-type contact process of α_0 = 10~15 deg which shows a high bonding rate. On the other hand, the Massif -type contact process of α_0 = 40~45 deg is controlled by both surface folding and interfacial expansion modes. Meanwhile, a low bonding rate is

achieved due to the constraint of contact process. The different contacting modes produce the effect of the void shape as a geometrical factor on the interfacial contact process and change the bonding rate.

4) The geometrical factor of surface roughness (void shape) can just influence the bonding process and it is independent to the bonding mechanism. In other words, even if the surface roughness changes, the identification of the predominant bonding mechanism is established.

In Chapter 5, the solid state bonding of superplastic steel and original steed in the finial bonding stage was investigated. The bonding process controlled by diffusion mechanisms was identified and two fundamental diffusional mechanisms were also discussed. The following points were clarified.

1) Diffusional creep predominantly contributes to the interfacial contact process from a bonding ratio of 65% to 72%, under the conditions of relatively low bonding pressure P = 10~20 MPa and bonding temperature T = 1023~1083K.
2) If the diffusional mechanism is predominant, the value of n is equal to unity and it can be less than unity due to the flattening of void shape.
3) The diffusion type can be also distinguished by the activation energy Q value. In other words, the value of Q is much close to Q_b when the grain boundary self-diffusion dominates. While the value of Q is much close to Q_v in the case of volume self-diffusion based Newtonian deformation is predominant.
4) For the solid state bonding between superplastic steel and original high carbon steel, the bonding mechanism under low bonding pressures can be controlled by diffusional creep and influenced by grain size of the original steel. The predominant bonding mechanism depends on the combined effect of both bonding materials.

5) Even though the bonding materials can show superplasticity behavior and the superplastic flow can occur during the bonding process, the diffusional bonding mechanisms are predominate in the final bonding stage for a sound bond.

A further discussion on the solid state bonding of superplastic materials is necessary. In general, the superplastic solid state bonding was produced under appropriate bonding conditions and it was confirmed by the characteristic values of *n*, and *Q*. The influences of surface roughness and material microstructure on the bonding process were also discussed in the present study.

However, superplastic flow cannot always predominantly contribute to the bonding process. It just acts on the interfacial contact process in the middle bonding stage when the interfacial stress is appropriate. There are still three unfinished points needed to be research in the next step.

Firstly, the interfacial stress contributed to the void shrinkage should be analyzed clearly. The stress distribution at the bonding interface is critical to the superplastic flow during the bonding process. The maximization of effect of superplastic flow can be achieved by adjusting the bonding pressures. That is, more efficient solid state bonding controlled by superplastic deformation can be obtained.

Next, the bonding process, especially bonding rate, is greatly influenced by the contact modes produced by the geometrical factor of surface roughness. The prediction of bonding time required to attain a sound bond is possible under different bonding conditions of surface roughness. The bonding process can be optimized further on the basis that the predominant bonding mechanism is established.

Finally, the present study is based on the solid state bonding between dissimilar

materials (superplastic steel and non-superplastic steel). As described in Chapter 5, the bonding process including the predominant bonding mechanism can be influenced by the bonding material. Considering the solid state bonding between superplastic materials, a more comprehensive description of bonding process is needed.

Acknowledgement

First of all, I would like to extend my sincere gratitude to my supervisor, Prof. Yasuo Takahashi, for his instructive advice and critical suggestion on my thesis. I am deeply grateful of his constant encouragement and guidance.

Second, I express my heartfelt gratitude to the professors at the Department of Materials and Manufacturing Science: Prof. Akio Hirose and Prof. Kazuyoshi Saida, who have instructed and helped me a lot in the completion of this thesis.

I am also greatly indebted to Prof. Masakatsu Maeda, Prof. Keke Zhang, Mr. Riki Horinouchi, Mr. Aiman, Mr. Yusuke Nashiki, Mr. Touma Matsushima, Mr. Kenji Ideguchi, and so many teachers, classmates and friends, in recent and past of the joining and welding research institute. In many tough situations during my research, they have advised and supported me so much.

Finally, special thanks should go to my parents and family for their loving considerations and great confidence in me all through these years.

Achievements

[1] Z. H. Heng, M. Maeda and Y. Takahashi: IOP Conf. Series: Mater. Sci. Eng., Doc.No. 61(2014)012003.

[2] Z. H. Heng, T. Matsushima, Y. Nashiki, M. Maeda, K. K. Zhang and Y. Takahashi: Quarterly Journal of the Japan Welding Society., 2015, Vol. 33(2), pp. 67-70.

[3] Z. H. Heng, T. Matsushima, Y. Nashiki, M. Maeda and Y. Takahashi: Journal of Smart Processing., 2015, Vol. 4, pp. 102-108.

[4] K. K. Zhang, Z. H. Heng, R. F. Qiu, H. X. Shi and Y. Takahashi: IOP Conf. Series: Mater. Sci. Eng., Doc.No. 61(2014) 012002